



Contents lists available at ScienceDirect

## Remote Sensing of Environment

journal homepage: [www.elsevier.com/locate/rse](http://www.elsevier.com/locate/rse)

## The EnMAP spaceborne imaging spectroscopy mission: Initial scientific results two years after launch

Sabine Chabrillat<sup>a,b,\*</sup>, Saskia Foerster<sup>a,y</sup>, Karl Segl<sup>a</sup>, Alison Beamish<sup>a</sup>, Maximilian Brell<sup>a</sup>, Saeid Asadzadeh<sup>a</sup>, Robert Milewski<sup>a</sup>, Kathrin J. Ward<sup>a</sup>, Arlena Brosinsky<sup>a</sup>, Katrin Koch<sup>a</sup>, Daniel Scheffler<sup>a</sup>, Stephane Guillaso<sup>a</sup>, Alexander Kokhanovsky<sup>a</sup>, Sigrid Roessner<sup>a</sup>, Luis Guanter<sup>c</sup>, Hermann Kaufmann<sup>a</sup>, Nicole Pinnel<sup>d</sup>, Emiliano Carmona<sup>d</sup>, Tobias Storch<sup>d</sup>, Tobias Hank<sup>e</sup>, Katja Berger<sup>a,k</sup>, Mathias Woher<sup>e</sup>, Patrick Hostert<sup>f</sup>, Sebastian van der Linden<sup>g</sup>, Akpona Okujeni<sup>a,f</sup>, Andreas Janz<sup>f</sup>, Benjamin Jakimow<sup>f</sup>, Astrid Bracher<sup>h,i</sup>, Mariana A. Soppa<sup>h</sup>, Leonardo M.A. Alvarado<sup>d,h</sup>, Henning Buddenbaum<sup>j</sup>, Birgit Heim<sup>h</sup>, Uta Heiden<sup>d</sup>, Jose Moreno<sup>k</sup>, Cindy Ong<sup>l</sup>, Niklas Bohn<sup>m</sup>, Robert O. Green<sup>m</sup>, Martin Bachmann<sup>d</sup>, Raymond Kokaly<sup>n</sup>, Martin Schodlok<sup>o</sup>, Thomas H. Painter<sup>p</sup>, Ferran Gascon<sup>q</sup>, Fabrizia Buongiorno<sup>r</sup>, Matti Mottus<sup>s</sup>, Vittorio Ernesto Brando<sup>t</sup>, Hannes Feilhauer<sup>u,x</sup>, Matthias Betz<sup>v</sup>, Simon Baur<sup>v</sup>, Rupert Feckl<sup>v</sup>, Anke Schickling<sup>q,w</sup>, Vera Krieger<sup>w</sup>, Michael Bock<sup>w</sup>, Laura La Porta<sup>w</sup>, Sebastian Fischer<sup>w</sup>

<sup>a</sup> Helmholtz Center Potsdam, GFZ German Research Center for Geosciences, Telegrafenberg, 14473 Potsdam, Germany

<sup>b</sup> Leibniz University Hannover, Institute of soil science, 30419 Hannover, Germany

<sup>c</sup> Universitat Politècnica de Valencia, Research Institute of Water and Environmental Engineering (IIAMA), 46022 Valencia, Spain

<sup>d</sup> German Aerospace Center (DLR), Earth Observation Center (EOC), 82234 Weßling, Germany

<sup>e</sup> Ludwig-Maximilians-Universität München (LMU), Dept. of Geography, 80333 Munich, Germany

<sup>f</sup> Humboldt-Universität zu Berlin, Geography Department, Unter den Linden 6, 10099 Berlin, Germany

<sup>g</sup> University of Greifswald, Institute for Geography and Geology, 17489 Greifswald, Germany

<sup>h</sup> Alfred Wegener Institute Helmholtz Centre for Polar and Marine Research, 27570 Bremerhaven, Germany

<sup>i</sup> University of Bremen, Institute of Environmental Physics, 28359 Bremen, Germany

<sup>j</sup> Trier University, Environmental Remote Sensing and Geoinformatics, 54286 Trier, Germany

<sup>k</sup> Laboratory for Earth Observation (LEO), Image Processing Laboratory (IPL), University of Valencia, 46980 Paterna, Valencia, Spain

<sup>l</sup> Commonwealth Scientific and Industrial Research Organisation (CSIRO), Bentley, WA, Australia

<sup>m</sup> Jet Propulsion Laboratory, California Institute of Technology, Pasadena, 91011 CA, USA

<sup>n</sup> U.S. Geological Survey (USGS), Geology, Geophysics, and Geochemistry Science Center, Lakewood, 80225 CO, USA

<sup>o</sup> Bundesanstalt für Geowissenschaften und Rohstoffe (BGR), Geozentrum Hannover, Germany

<sup>p</sup> Department of Geography, Joint Institute for Regional Earth System Science and Engineering, 9258 Boelter Hall, Los Angeles, USA

<sup>q</sup> European Space Agency (ESA), 00044 Frascati, Italy

<sup>r</sup> National Institute of Geophysics and Volcanology (INGV), 00143 Rome, Lazio, Italy

<sup>s</sup> Technical Research Centre of Finland (VTT), 02044 Espoo, Finland

\* Corresponding author at: Helmholtz Center Potsdam, GFZ German Research Center for Geosciences, 14473 Potsdam, Germany.

E-mail addresses: [sabine.chabrillat@gfz-potsdam.de](mailto:sabine.chabrillat@gfz-potsdam.de) (S. Chabrillat), [saskia.foerster@uba.de](mailto:saskia.foerster@uba.de) (S. Foerster), [karl.segl@gfz-potsdam.de](mailto:karl.segl@gfz-potsdam.de) (K. Segl), [alison.beamish@gfz-potsdam.de](mailto:alison.beamish@gfz-potsdam.de) (A. Beamish), [maximilian.brell@gfz-potsdam.de](mailto:maximilian.brell@gfz-potsdam.de) (M. Brell), [saeid.asadzadeh@gfz-potsdam.de](mailto:saeid.asadzadeh@gfz-potsdam.de) (S. Asadzadeh), [robert.milewski@gfz-potsdam.de](mailto:robert.milewski@gfz-potsdam.de) (R. Milewski), [kathrin.ward@gfz-potsdam.de](mailto:kathrin.ward@gfz-potsdam.de) (K.J. Ward), [arlena.brosinsky@gfz-potsdam.de](mailto:arlena.brosinsky@gfz-potsdam.de) (A. Brosinsky), [katrin.koch@gfz-potsdam.de](mailto:katrin.koch@gfz-potsdam.de) (K. Koch), [daniel.scheffler@gfz-potsdam.de](mailto:daniel.scheffler@gfz-potsdam.de) (D. Scheffler), [stephane.guillaso@gfz-potsdam.de](mailto:stephane.guillaso@gfz-potsdam.de) (S. Guillaso), [alexander.kokhanovsky@gfz-potsdam.de](mailto:alexander.kokhanovsky@gfz-potsdam.de) (A. Kokhanovsky), [sigrid.roessner@gfz-potsdam.de](mailto:sigrid.roessner@gfz-potsdam.de) (S. Roessner), [lguanter@fis.upv.es](mailto:lguanter@fis.upv.es) (L. Guanter), [nicole.pinnel@dlr.de](mailto:nicole.pinnel@dlr.de) (N. Pinnel), [emiliano.carmona@dlr.de](mailto:emiliano.carmona@dlr.de) (E. Carmona), [tobias.storch@dlr.de](mailto:tobias.storch@dlr.de) (T. Storch), [tobias.hank@lmu.de](mailto:tobias.hank@lmu.de) (T. Hank), [katja.berger@gfz-potsdam.de](mailto:katja.berger@gfz-potsdam.de) (K. Berger), [m.wocher@iggf.geo.uni-muenchen.de](mailto:m.wocher@iggf.geo.uni-muenchen.de) (M. Woher), [patrick.hostert@geo.hu-berlin.de](mailto:patrick.hostert@geo.hu-berlin.de) (P. Hostert), [sebastian.linden@uni-greifswald.de](mailto:sebastian.linden@uni-greifswald.de) (S. van der Linden), [akpona.okujeni@gfz-potsdam.de](mailto:akpona.okujeni@gfz-potsdam.de) (A. Okujeni), [andreas.janz@geo.hu-berlin.de](mailto:andreas.janz@geo.hu-berlin.de) (A. Janz), [benjamin.jakimow@geo.hu-berlin.de](mailto:benjamin.jakimow@geo.hu-berlin.de) (B. Jakimow), [astrid.bracher@awi.de](mailto:astrid.bracher@awi.de) (A. Bracher), [msoppa@awi.de](mailto:msoppa@awi.de) (M.A. Soppa), [leonardo.alvarado@dlr.de](mailto:leonardo.alvarado@dlr.de) (L.M.A. Alvarado), [buddenbaum@uni-trier.de](mailto:buddenbaum@uni-trier.de) (H. Buddenbaum), [birgit.heim@awi.de](mailto:birgit.heim@awi.de) (B. Heim), [uta.heiden@dlr.de](mailto:uta.heiden@dlr.de) (U. Heiden), [jose.moreno@uv.es](mailto:jose.moreno@uv.es) (J. Moreno), [cindy.ong@csiro.au](mailto:cindy.ong@csiro.au) (C. Ong), [urs.n.bohn@jpl.nasa.gov](mailto:urs.n.bohn@jpl.nasa.gov) (N. Bohn), [robert.o.green@jpl.nasa.gov](mailto:robert.o.green@jpl.nasa.gov) (R.O. Green), [martin.bachmann@dlr.de](mailto:martin.bachmann@dlr.de) (M. Bachmann), [raymond@usgs.gov](mailto:raymond@usgs.gov) (R. Kokaly), [martin.schodlok@bgr.de](mailto:martin.schodlok@bgr.de) (M. Schodlok), [tpainter@jifresse.ucla.edu](mailto:tpainter@jifresse.ucla.edu) (T.H. Painter), [ferran.gascon@esa.int](mailto:ferran.gascon@esa.int) (F. Gascon), [fabrizia.buongiorno@ingv.it](mailto:fabrizia.buongiorno@ingv.it) (F. Buongiorno), [matti.mottus@vtt.fi](mailto:matti.mottus@vtt.fi) (M. Mottus), [vittorio.brande@cnr.it](mailto:vittorio.brande@cnr.it) (V.E. Brando), [hannes.feilhauer@uni-leipzig.de](mailto:hannes.feilhauer@uni-leipzig.de) (H. Feilhauer), [matthias.betz@ohb.de](mailto:matthias.betz@ohb.de) (M. Betz), [simon.baur@ohb.de](mailto:simon.baur@ohb.de) (S. Baur), [rupert.feckl@ohb.de](mailto:rupert.feckl@ohb.de) (R. Feckl), [anke.schickling@esa.int](mailto:anke.schickling@esa.int) (A. Schickling), [vera.krieger@dlr.de](mailto:vera.krieger@dlr.de) (V. Krieger), [michael.bock@dlr.de](mailto:michael.bock@dlr.de) (M. Bock), [laura.laporta@dlr.de](mailto:laura.laporta@dlr.de) (L. La Porta), [sebastian.fischer@dlr.de](mailto:sebastian.fischer@dlr.de) (S. Fischer).

<https://doi.org/10.1016/j.rse.2024.114379>

Received 2 February 2024; Received in revised form 30 July 2024; Accepted 19 August 2024

0034-4257/© 2024 The Authors. Published by Elsevier Inc. This is an open access article under the CC BY license (<http://creativecommons.org/licenses/by/4.0/>).

<sup>†</sup> Consiglio Nazionale delle Ricerche, Istituto di Scienze Marine (CNR-ISMAR), 30122 Rome, Italy

<sup>‡</sup> Leipzig University, Remote Sensing Centre for Earth System Research, 04103 Leipzig, Germany

<sup>§</sup> OHB System AG, 82234 Wessling, Germany

<sup>¶</sup> German Aerospace Center (DLR), German Space Agency, 53227 Bonn, Germany

<sup>\*\*</sup> Helmholtz Centre for Environmental Research - UFZ Leipzig, 04318 Leipzig, Germany

<sup>††</sup> Umweltbundesamt (UBA) - German Environment Agency, Wörlitzer Platz 1, 06844 Dessau-Roßlau, Germany

## ARTICLE INFO

Edited by Jing M. Chen

## Keywords:

EnMAP mission

Space-based imaging spectroscopy

VNIR-SWIR

Science cases

Surface and atmosphere

Bio-geochemical mapping

## ABSTRACT

Imaging spectroscopy has been a recognized and established remote sensing technology since the 1980s, mainly using airborne and field-based platforms to identify and quantify key bio- and geo-chemical surface and atmospheric compounds, based on characteristic spectral reflectance features in the visible-near infrared (VNIR) and short-wave infrared (SWIR). Spaceborne missions, a leap in technology, were sparse, starting with the CHRIS/PROBA and EO1/Hyperion missions in the early 2000s, and providing spectroscopy data with limited spectral coverage and/or low data quality in the SWIR. Since 2019, several countries and agencies have successfully launched a number of spaceborne imaging spectroscopy systems into orbit or deployed them on the International Space Station (ISS) such as DESIS, PRISMA, HISUI, GF-5, EnMAP and EMIT. Among these recent missions, the German Environmental Mapping and Analysis Program (EnMAP) stands for its long-term development, sophisticated design with on-board calibration, high data quality requirements, and extensive accompanying science program. EnMAP was launched in April 2022 and, following a successful commissioning phase, started its operational activities in November 2022. The EnMAP mission encompasses global coverage from 80° N to 80° S through on-demand data acquisitions. Data are free and open access with 30 m spatial resolution, a high spectral resolution with a spectral sampling distance of 6.5 nm and 10 nm in the VNIR and SWIR regions respectively, and a high signal-to-noise ratio. In this paper, we aim to present the mission's current status, coverage, science capabilities and performance two years after launch. We show the potential of EnMAP for space-based imaging spectroscopy to operate in various environments, including high and low light levels, dense forests, Antarctic glaciers, and arid agricultural areas. EnMAP enables various applications in fields such as agriculture and forestry, soil compositional, raw materials, and methane mapping, as well as water quality assessment, and snow and ice properties. The results show that EnMAP's performance exceeds the mission requirements, and highlights the significant potential for contribution to scientific exploitation in various geo- and biochemical sciences. EnMAP is also expected to serve as a key tool for the development and testing of data processing algorithms for upcoming global operational missions.

## 1. Introduction

Nowadays, sustainable development of the Earth's natural resources is a serious health and life matter. The 2030 Agenda for Sustainable Development, adopted by all United Nations Member States in 2015, provides a shared blueprint for peace and prosperity for people and the planet, now and into the future. At its core are the 17 Sustainable Development Goals (SDGs), which are an urgent call for action by all countries - developed and developing - in a global partnership (UN, 2016). They recognize that ending poverty and other deprivations must go hand-in-hand with strategies that improve health and education, reduce inequality, and spur economic growth – all while tackling climate change and working to preserve our oceans and terrestrial ecosystems. In this context, global mapping and monitoring of our environment based on Earth observation platforms serve as the foundation for evaluating our planet's health and development, for identifying and managing natural resources to support their sustainable exploitation, and to ensure food security. Estimation of carbon fluxes is a critically important and rapidly evolving topic in the context of climate change, and assessment of carbon emissions and carbon storage in soils, vegetation and water bodies will provide a more detailed estimation for carbon cycle modeling (Araza et al., 2023; Brewin et al., 2023; Xiao et al., 2019). Snow, sea ice, permafrost and ice fields are retreating and the resulting exposed high-altitude and latitude land surfaces reflect environmental changes that need to be quantified (AMAP, 2017; Duncan et al., 2020; van den Broeke et al., 2017).

Reflectance spectroscopy in the VNIR and SWIR ranging from 400 to 2500 nm has been a key technology for many decades for characterization, identification, and quantification of surface and atmospheric compositions in multiple environments, being an indispensable instrument for an improved knowledge of Earth surface properties and processes, their dynamics and evolution (Goetz et al., 1985; Schaepman et al., 2009). The spectral reflectance of surface materials recorded in

the spectrally contiguous, narrow bands of imaging spectrometers provides diagnostic information on a wide range of relevant biogeochemical and atmospheric parameters (Clark, 1999; Guanter et al., 2008). While airborne platforms have been used since the early 1980s, the development of spaceborne platforms has been a technological challenge resulting in a limited number of spaceborne systems up to now.

Spaceborne imaging spectroscopy has a wide range of applications, encompassing soils and mining, agriculture and forestry, water and snow, emissions, as well as anthropogenic and natural hazards, and can thus provide valuable information for monitoring and managing Earth's resources. It allows for quantitative measurements of the biochemical and physical characteristics of terrestrial, aquatic, and atmospheric Earth systems' components based on calibrated spectra acquired as images (Goetz, 2009; Schaepman et al., 2009). Thus, spaceborne imaging spectroscopy data will help improving our understanding of Earth's surface processes and address major environmental challenges related to human activities and climate change (Guanter et al., 2015). It will improve the mapping of the Earth surface with unprecedented accuracy and detail, contributing to Earth system science and enhanced ecosystem modeling.

Spatial and spectral information derived from imaging spectroscopy missions has the potential to benefit a range of international policies and programs, such as the International Geosphere-Biosphere Program (IGBP) and the United Nations Sustainable Development Goals (SDGs). Also the new surface and atmospheric products will support organizations like the United Nations Global Climate Observing System (GCOS), environmental agreements such as the United Nations program for Reducing Emissions from Deforestation and forest Degradation in developing countries (REDD+) or the Convention to Combat Desertification (UNCCD), and international programs and observatories such as the Intergovernmental Panel on Climate Change (IPCC), exemplified by its role in UNEP's International Methane Emissions Observatory (IMEO). At the European Union level, spaceborne imaging spectroscopy data are

going to be an essential support for the European Green Deal and various Commission directorates, informing policies like the EU Water Framework Directive (EU, 2000) and the New European Union Soil Strategy for 2030 (EU, 2021).

Over the past three decades, substantial efforts have been dedicated to developing imaging spectrometers capable of acquiring continuous spectra across the VNIR and SWIR wavelength ranges. These instruments, like AIS, CASI, AVIRIS, GER/DAIS and others (please see full list of manuscript abbreviations in supplementary materials, Table B.1), were primarily deployed on airborne platforms for both experimental and commercial purposes. However, aircraft-based data acquisition has limitations, including the inability to provide comprehensive coverage of large areas and the high cost associated with repeat acquisitions. Following HYPERION and CHRIS precursor missions (Barnsley et al., 2004; Pearlman et al., 2003), the availability of spaceborne imaging spectroscopy data has significantly increased recently with the successful launches of several satellite missions such as Gaofen-5 (2018) (Liu et al., 2019), PRISMA (2019) (Lopinto et al., 2022), and EnMAP (2022) (Storch et al., 2023). In addition to these satellites, imaging spectrometers have been installed on the International Space Station (ISS), including DESIS (2018) (Alonso et al., 2019), HISUI (2019) (Matsunaga et al., 2022) and EMIT (2022) (Green, 2022). Future imaging spectroscopy missions, such as ESA's CHIME (Celesti et al., 2022) and NASA's SBG (Turpie et al., 2023) planned to be launched by the end of the 2020s, represent the next generation of operational hyperspectral imaging satellite missions. They will advance capabilities for Earth observation and environmental analysis to a global and frequent acquisition of the Earth's surface.

EnMAP was launched into space on 1st April 2022 and started routine operations in November 2022 (Storch et al., 2023). The mission aims to provide high-quality calibrated imaging spectroscopy data for advanced remote sensing analyses and to develop novel methodologies to improve the type and accuracy of currently available remote sensing information (Chabrilat et al., 2022). The mission also seeks to investigate globally interconnected environmental processes and changes, study the diverse effects of human interventions on ecosystems, and measure, derive, and analyze qualitative and quantitative diagnostic surface variables. Overall, the EnMAP mission provides unique data needed to address major environmental challenges related to human activities and climate change, and significantly increases the availability of hyperspectral measurements over the Earth.

EnMAP represents a pioneering mission in the realm of global imaging spectroscopy mapping in several aspects related to its long-term preparation, to the incorporation of on-board calibration to ensure data quality and accuracy, and to the science program and development including external validation efforts. Comprehensive atmospheric correction techniques are applied to address land, water, and combined scenarios. The mission is characterized by user-driven acquisition strategies and offers substantial scientific support, including software development and educational programs, and simulation packages. Over the past years, its open data and open science policy has promoted accessibility and transparency by providing, for the first time, open and free data and tools exclusively focusing on imaging spectroscopy science and algorithms, including resources like the EnMAP-Box (Van Der Linden et al., 2015; Jakimow et al., 2023) and HYPERedu (Foerster et al., 2024) supporting imaging spectroscopy data analyses and education.

The EnMAP mission consortium is a collaborative effort led by the German Space Agency at the German Aerospace Center (Deutsches Zentrum für Luft- und Raumfahrt; DLR) in Bonn, primarily funded by the Federal Ministry of Economic Affairs and Climate Action. The science segment is led by the German Research Centre for Geosciences (GFZ) in Potsdam, with support from an international Science Advisory Group (EnSAG). OHB SE in Bremen and Oberpfaffenhofen played pivotal roles in developing the EnMAP instrument and constructing the associated satellite platform. The ground segment operations are managed by DLR

in Oberpfaffenhofen, with satellite operations handled by the German Space Operations Center, and data processing and provisioning managed by the German Remote Sensing Data Center and the DLR Remote Sensing Technology Institute.

The aim of this paper is to provide an initial assessment of EnMAP data quality and science results two years after launch. For this, first we will provide a concise overview of the EnMAP mission's current status, covering its objectives, orbit and sensor characteristics, acquisitions and users interests, current quality assurance performance and data products, with the inclusion of science algorithm development and training activities (provided in Supplementary materials). Then we will showcase EnMAP's quality and potential in a range of application fields such as soil and mineral mapping, agriculture and forestry, water monitoring, snow and ice environments, methane detection, and hazard assessment. This will be demonstrated through case studies based on current acquired EnMAP imagery. Finally, we explore the mission's synergies, highlighting its pioneering role in spaceborne imaging spectroscopy, international collaborations, open data initiatives, and higher-level product development for improved land and water management.

## 2. EnMAP Mission overview

### 2.1. Mission objectives

The main scientific goal of the hyperspectral EnMAP mission is to study environmental changes, investigate ecosystem responses to human activities, and monitor the management of natural resources. By measuring diagnostic parameters of environmental change, ecosystem stability, and sustainable resource use, the EnMAP mission aims to provide critical information to improve our understanding and management of the Earth System.

More specifically, the primary science mission objectives of EnMAP are defined as follows (Chabrilat et al., 2022):

- provide high-quality, calibrated hyperspectral data for advanced remote sensing analyses;
- foster and develop novel methodologies that improve the accuracy of currently available remote sensing-derived information and provide advanced science-driven information products;
- obtain diagnostic geochemical, biochemical, and biophysical variables that describe the status and dynamics of various ecosystems to improve our understanding of complex environmental processes;
- provide information products that can serve as input for ecosystem models;
- contribute significantly to environmental research studies, particularly in the fields of ecosystem functioning, natural resource management, natural hazards, and Earth system modeling; and
- develop new concepts and techniques for data extraction and fusion to achieve synergies with other sensors.

One of the priority of the science objectives of the EnMAP mission, during both the preparatory and operational phase, was the development of free and open-source data processing tools, as well as an educational program to further foster the evolution of an expert user community (Foerster et al., 2016). Two of the major outcomes of these efforts have been used worldwide since many years. These are the EnMAP-Box toolbox (Jakimow et al., 2023) and the HYPERedu education program (Foerster et al., 2024), whose current status are displayed in the Supplementary materials (please refer to appendices A.1 and A.2 for more details). Both programs comprise 5 to 10 years of conceptualization and implementation and are now online for many years. Their development will continue into the future, including the integration of adapted as well as new algorithms, and the release of innovative, state-of-the-art educational resources.

Overall, EnMAP's goal is to significantly increase the availability of imaging spectroscopy data, to drive the development of novel

techniques to improve the analysis of imaging spectroscopy coverage from the regional to the global scale, and to extrapolate based on multi-scale reflectance data derived from laboratory, field, and airborne measurements. The integration of these data into regional ecosystem models will complement, enhance, and expand on local case study findings and will improve regional-scale science on the state and change of ecosystems for improved global ecosystem models. Such upscaling studies require calibration, consolidation and generalization or globalization of the derived ecosystem parameters, linked with synergistic analyses with other spaceborne imagery like ESA's Copernicus satellites. Due to the 30° across track off-nadir pointing capability, EnMAP is furthermore suited for repeat acquisitions of target sites with a minimum revisit time of four days. Considering the cloud occurrence, it increases the opportunity of repeatedly observing locations (in case of a disaster or for very dynamic environments such as coastal zones). With a nominal revisit time of 27 days, EnMAP allows to repeatedly observe a globally distributed network of key target sites over the mission lifetime.

## 2.2. Sensor and orbit

The payload aboard the EnMAP satellite includes a VNIR-SWIR push-broom hyperspectral imager covering the nominal range of 420-2450 nm with 224 contiguous bands. The sensor has a spectral sampling distance of 6.5 nm in the VNIR and 10 nm in the SWIR, with a ground sampling distance of 30 m and a swath width of 30 km. VNIR and SWIR lines-of-sight are separated by a distance of ~600 m on the ground and the data is being resampled to a common grid after geometric processing. EnMAP has a sun-synchronous orbit with a nominal revisit time of 27 days. Off-nadir pointing capabilities up to 30° can reduce the revisit time up to four days for fast target revisit. For a more detailed description of the technical parameters see (Guanter et al., 2015; Kaufmann et al., 2015; Storch et al., 2023). Please note that the co-registration VNIR-SWIR was set up from requirements at 26% along-track and 30% across-track of the pixel size. These values have been decreasing

**Table 1**  
EnMAP technical parameters requirements.

Hyperspectral instrument	
Imaging principle	Push broom prism
Spectral range	VNIR: 420 nm – 1000 nm SWIR: 900 nm – 2450 nm
Mean spectral sampling distance	VNIR: 6.5 nm SWIR: 10 nm
Spectral oversampling	1.2
SNR at reference radiance	VNIR: > 400:1 at 495 nm (nadir looking, 30° solar zenith angle) SWIR: > 170:1 at 2200 nm (0.3 earth albedo)
Spectral calibration accuracy	VNIR: 0.5 nm SWIR: 1.0 nm
Spectral stability	0.5 nm
Radiometric calibration accuracy	< 5 %
Radiometric stability	< 2.5 %
Radiometric resolution	14-bit, dual gain in VNIR
Sensitivity to polarization	< 5 %
Spectral smile/keystone effect	< 20 % / < 20 % of a pixel (Achieved <10 % / < 10 % for majority of pixels)
Co-registration VNIR-SWIR	30%. Achieved <12% after 29.03.2023
<b>Mission</b>	
Ground sampling distance	30 m
Swath width	30 km
Swath length	up to 1000 km/orbit and 5000 km/day
Coverage	Global in near-nadir mode (VZA ≤5°)
Orbit	Sun-synchronous, 11:00 +/- 00:18 local time descending node
Target revisit time	27 days (4 days with 30° across track pointing)
Pointing accuracy (knowledge)	500 m (100 m) at sea level

over time up to the current ones amounting to <12% (see Table 1).

## 2.3. Data products, access, proposal and user statistics

The EnMAP ground segment provides the necessary services for satellite control and reception, storage, and processing of EnMAP data up to the three user product levels that can be ordered. These products comprise radiometrically corrected at sensor top-of-the-atmosphere radiance products (L1B), radiometrically corrected and orthorectified top-of-the-atmosphere radiance products (L1C), and the atmospherically and terrain-corrected bottom-of-the-atmosphere reflectance products (L2A). The L2A processing includes options for land and water processing, as well as a combined mode that automatically selects the correction based on pixel classification. All products are processed on-demand with up-to-date processor versions and radiometric as well as spectral calibration, while geometric calibration requires a re-processing of the archived L0 products from the raw data currently ongoing and that will be completed by the end of 2024. Additionally, extensive metadata and quality layers are included to ensure for the L2A land product the Analysis Ready Data conformity with CEOS CARD4L at the threshold level (Bachmann et al., 2021; Storch et al., 2023).

Users can order new acquisitions and access archived data through the EnMAP Instrument Planning portal (<https://planning.enmap.org/>). Data access is provided by submitting a short proposal for new acquisition requests, or by ordering archived data through the EOWEB® GeoPortal. All archived data adhere to International Organization for Standardization (ISO) metadata standards and can be visualized in the portal. Data are delivered to the user by secure file transfer protocol (SFTP). Acquisition priority is determined by user category as follows: 1) internal (high priority, e.g. calibration) (Priority 9); 2) emergency Cat-2 (Priority 8) (e.g. international charter on space and major disasters, foreground mission); 3) scientific Cat-1 (Priority 7) (high priority, science proposal); 4) scientific Cat-1 (Priority 6) (standard priority, science proposal); 5) non-emergency Cat-2 (Priority 5) (e.g. commercial users); and 6) scientific Cat-1 (Priority 4) (low priority, e.g., science proposal in 2023 with no or exceeded quota, background mission), and 7) internal (Priority 0) (lowest priority). For a more detailed description of data products, processing, and access see Storch et al. (2023). As a supplementary search tool, the EOLab platform (<https://eo-lab.org/de/>) provides an alternative means of locating Level 2A standardized EnMAP products, allowing users to filter searches based on temporal and spatial criteria.

The number of registered users has been increasing continuously since the start of the routine phase. As of June 30, 2024, there were a total of 2559 registered EnMAP users representing over 90 countries worldwide, 2006 of which are science users and 1975 catalogue users (some users have more than one user role). Since the launch in April 2022, 10,769 data takes have been performed resulting in 82,050 archived independent EnMAP tiles of 30 × 30 km (see also Table 2).

A total of 565 science proposals have been approved so far, which are assigned to three different Announcement of Opportunities (AO). The largest number of proposals comes from the vegetation applications, accounting for nearly 50% of all tiles granted, whereas the second highest number of proposal is focusing on geology/soil applications,

**Table 2**

Number of users per Category since mission start (01.04.2022 until 30.06.2024: (1) number of registered Users with at least one active user role, (2) number of Cat-1 Users and released Cat-1 User roles in total, (3) number of released proposals and (4) number of Catalogue users.

	User Category	Number
1	<b>User Registered (active)</b>	2559
2	<b>Cat-1 Users</b>	2006
3	<b>Proposals</b>	565
4	<b>Catalogue User</b>	1975

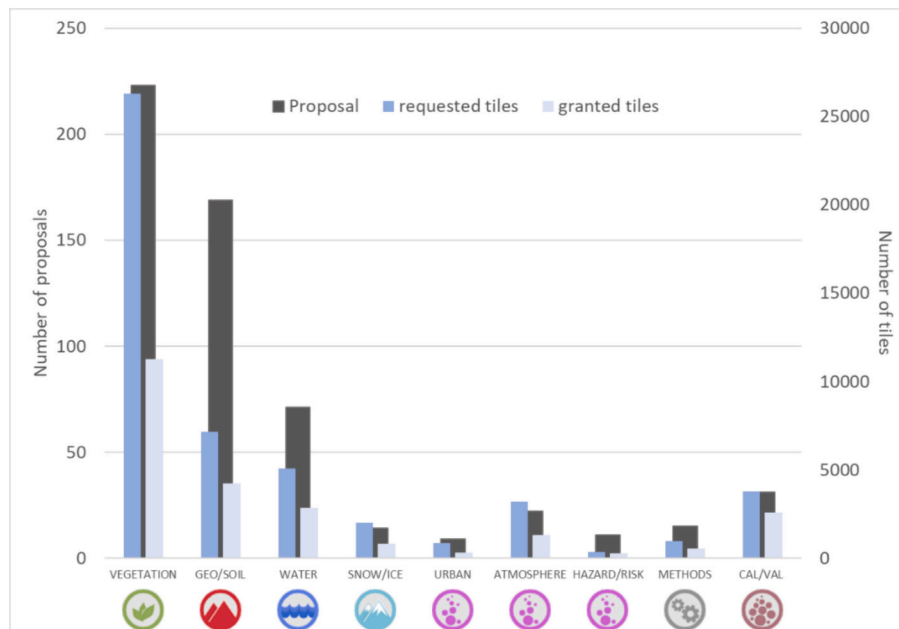


**Fig. 1.** Number of granted proposals per topic, and requested and granted tiles per topic since start of operational phase (02.11.2022 until 30.06.2024). The y-axis on the left shows the number of granted proposal per topic, whereas the y-axis on the right shows the number of requested and granted tiles per topic.

with ~17% of all tiles granted, followed by the water applications accounting for ~12% of all tiles granted. Then in decreasing order of number of proposals, comes cal/val (~11% of all granted tiles), atmosphere (~5%), methods, snow and ice applications, and finally hazards/risks and urban applications (~ < 1% of all tiles granted) (see Fig. 1).

Fig. 2 shows an analysis of EnMAP acquisitions, users acquisitions, users interest, and users spatial distribution. It includes a) a global map of all EnMAP data acquisitions, b) a global map of user-requested acquisitions vs. interest map (based on proposal targets), and c) a global map of registered users (with an active role) per country. The global acquisition pattern in Fig. 2a is highly non-uniform as it responds to both user requests and to background and foreground acquisitions derived by mission internal priorities and focusing on science core sites, but also with a mandate to fill up the mission capacity considering mapping missions demonstrations in remote regions of the Earth, where orbits are largely empty. User requests in general are associated with shorter acquisitions due to interest in mostly 1 or 2 tiles long acquisitions (shown in orange in Fig. 2b). Longer acquisition patterns are associated with background or foreground mission where typically ~20 (600 km) or ~33 tiles (1000 km long) acquisitions are acquired continuously on one orbit.

For a deeper study into the pattern of EnMAP acquisitions and the user interests towards EnMAP imaging spectroscopy data, Fig. 2b shows a global map of all EnMAP acquisitions based solely on user requests since 01 January 2023 (user acquisitions with 7 tiles or less, in orange) compared with user interest points (requested coordinated entered by the users in their proposals, in blueish). User interests are distributed over the five continents although with the highest concentration over Europe. On the other hand, blue circles signalize user interest points where no acquisitions could be made, although orange points locate areas where user requests were successfully acquired. Finally, Fig. 2c illustrates the global distribution of EnMAP users. Currently, the number of active registered users on the EnMAP portal from outside Europe is nearly equal to the number of European users.

### 3. EnMAP product quality

The EnMAP mission is dedicated to providing high-quality hyperspectral image data to derive information about the state of the environment and to monitor Earth's surface changes (Guanter et al., 2015). To adequately address the manifold scientific questions, the radiometric, spectral, geometric, and reflectance quality of the three EnMAP products (L1B, L1C, and L2A) are of central importance, as they significantly influence the analytical interpretability and quantifiability as well as the global generalizability and transferability of the derived results. Therefore, significant efforts are devoted to instrument calibration and product validation to ensure the required quality (Brell et al., 2021, 2022; Storch et al., 2023).

#### 3.1. EnMAP pre- and in-flight calibration and product validation

Adequate pre- and in-orbit instrument calibration and characterization is the backbone for high-quality EnMAP products. Extensive laboratory characterization and calibration at OHB-System AG before launch ensured the integrity, functionality, and fulfillment of the required specifications and, thus, flight qualification and readiness. EnMAP's advanced on-board calibration assembly is used in orbit to update the radiometric and spectral calibrations to accommodate the changing in-flight conditions and resulting challenges (Storch et al., 2023).

Besides the EnMAP ground segment (DLR) calibration and internal quality control activities, all provided product levels are validated continuously to ensure product quality and to meet the mission requirements. During the commissioning and operational phases, the EnMAP science segment (GFZ) leads the external validation efforts guided by the EnSAG from a scientific user perspective and supported by international collaborators (Brell et al., 2024; Brell et al., 2022). This task includes collaboration with the international community to build the EnMAP validation team acquiring in-situ measurements during EnMAP overpasses all over the world in different areas with varying surface and atmospheric conditions also pursuing the goal of

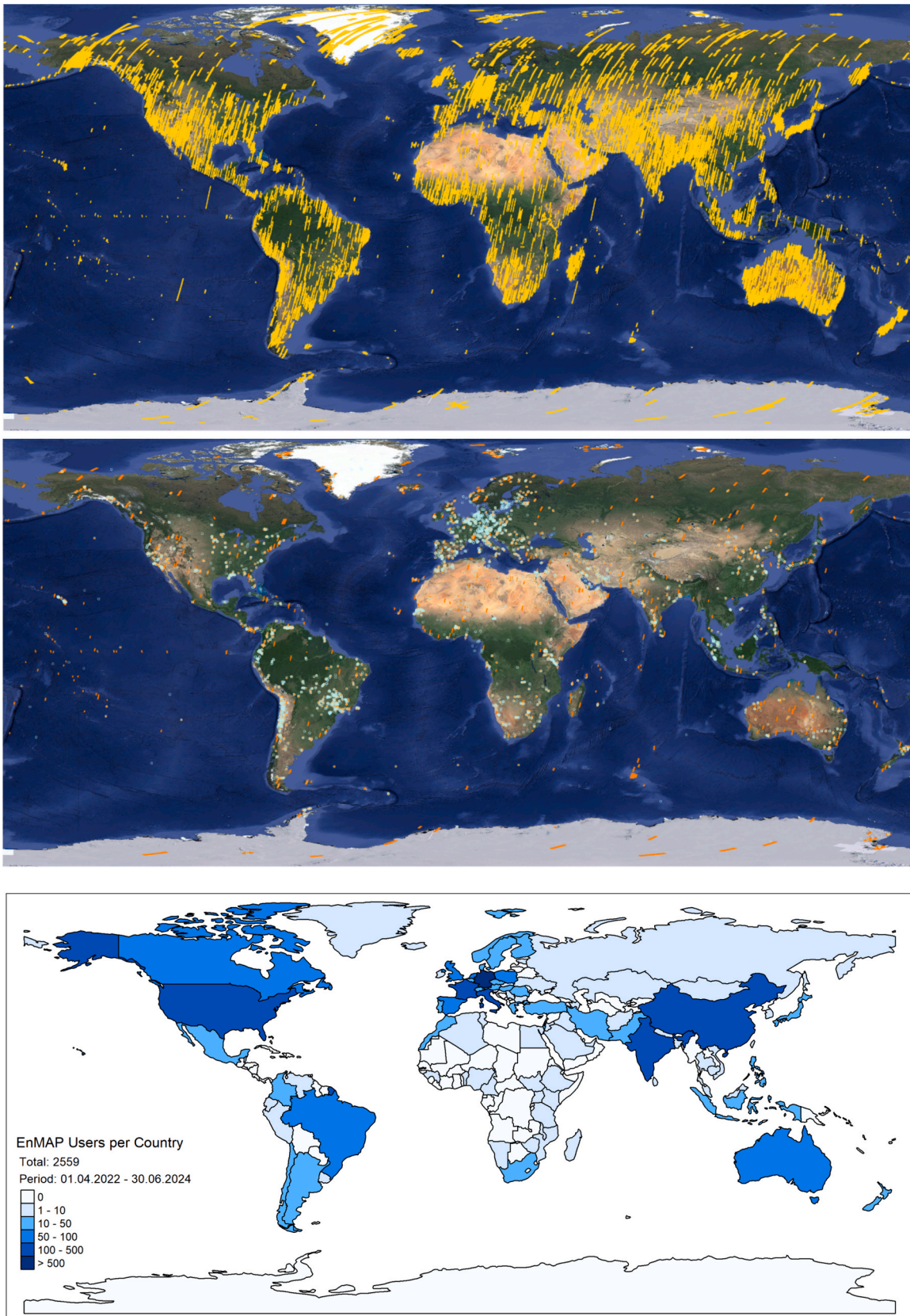


**Fig. 2.** a) (top) Global map of EnMAP data acquisitions from 01 April 2022 to 30 June 2024; b) (middle) Global map of EnMAP user acquisitions (orange) compared with user requested coordinates (blueish). (Map background data ©2023 Google. Data SIO, NOAA, U.S. Navy, NGA, GEBCO, Landsat / Copernicus, U.S. Geological Survey, IBCAO PGC/NASA. 30.11.1998–14.12.2015); c) (bottom) Global map of number of registered EnMAP users (with an active user role) per country.

**Table 3**  
Validated product parameters.

	Validated Parameters	Mission Requirements	Achieved
	Radiometric accuracy	5.0 %	≤ 5.0 %
L1B	Smile	< 20 % linear displacement of a detector element	VNIR (761 nm): 4.1% SWIR (2300 nm): 12.5 %
	SNR	VNIR >343:1 (@495 nm & SSD 4.7 & 30% reflective target) SWIR >137:1 (@2200 nm & SSD 8.4 & 30% reflective target)	354:1 260:1
L1C	Absolute geometric accuracy	< 1 GSD (if matching possible)	17.57 m in x 19.54 m in y
	Co-registration VNIR/SWIR	RMSE <30 % of a pixel	3.8 m in x 4.0 m in y
L2A – Land	BOA Reflectance	Uncertainty (RMSE) < 0.01 for reflectance <0.1 and < 0.02 for reflectance 0.1 ≤ ρ < 0.3 < 0.05 for reflectance 0.3 ≤ ρ ≤ 0.6 Uncertainty (RMSE) For AOT at 550 nm < 0.4: < 0.04 for 400 nm < λ ≤ 450 nm < 0.02 for 450 nm < λ ≤ 650 nm < 0.01 for 650 nm < λ ≤ 800 nm	fulfilled
L2A – Water	Normalized Water Leaving Reflectance	For AOT at 550 nm > 0.4: < 0.05 for 400 nm < λ ≤ 450 nm < 0.03 for 450 nm < λ ≤ 650 nm < 0.02 for 650 nm < λ ≤ 800 nm	fulfilled

For clear water pixels outside sunglint contaminated areas

cross-validation with other current optical and hyperspectral spaceborne missions (e.g., Sentinel-2, PRISMA, EMIT, DESIS). To control and monitor the validity and quality of calibrations and the derived products during the operational phase, the efforts of GFZ and the international partners continue to provide external validation and monitoring activities (Brell et al., 2024; Brell et al., 2023).

The overall validation and quality investigations in the commissioning and following years of the operational phase indicate that all mission requirements have been satisfactorily fulfilled and are well beyond the original requirements (see Table 3), with the potential to further improve and create new fields of science applications.

Some minor issues were identified, which were addressed or fixed during the early operational phase. Accordingly, users shall make sure to obtain EnMAP data processed after 29 March 2023 (processor versions after V01.02.00) since it includes major quality improvements regarding radiometric sensor stability and degradation, across-track striping, VNIR-SWIR co-registration, absolute geometric quality, and the unmasking of several bands close to the strong water vapor regions. For best performance, it is generally recommended to use the most recent processing version. In particular, geology users shall make use of EnMAP data processed after 05 July 2023 due to changes in the provided EnMAP band set to add important geological wavelengths close to atmospheric bands (e.g. at 1750-1770 nm). Furthermore, the re-processing of archived products (L0 reprocessing for improved geometric calibration) systematically started for all archived products prior to 24.08.2023. A version number equal to or higher than V01.03.00 will identify a re-processed product. Overall, for best performance, it is generally recommended to use the latest archived version when more than one version of the product exists. Based on the intensive calibration and validation activities, the quality of the EnMAP products is guaranteed and constantly improved. Finally, the EnMAP data quality has shown to be well beyond the mission requirements.

### 3.2. EnMAP reflectance examples

The primary product of interest for EnMAP users is the orthorectified bottom-of-atmosphere reflectance (EnMAP L2A product). Fig. 3 shows characteristic EnMAP reflectance spectra for selected scientific applications. The spectra indicate that the product quality of EnMAP is excellent, and all essential distinctive features for the respective applications are represented. Due to the high data quality and low noise from the VNIR to the SWIR spectral region, the demanding requirements from various scientific application areas ranging from low to high reflectance and narrow and weak absorption features are met by EnMAP and allow scientific applications for a wide range of thematic topics.

More details about the EnMAP product quality and parameter validation can be found in Storch et al. (2023) and in the mission quarterly reports at <https://www.enmap.org/mission/>. More detailed information on EnMAP validation results and methods can be found in (Brell et al., 2021, 2022).

## 4. Scientific applications

To effectively address the most pressing environmental challenges facing planet Earth, accurate and quantitative information about bio-, geo-, hydro- and atmosphere is needed. Below we demonstrate a few specific EnMAP-based case studies, the first results, and the potential to support science applications in the field of quantitative characterization of Earth surface properties while making use of the exceptionally high quality of the EnMAP data. Examples range from low radiance levels (water applications, volcanic areas) to high radiance levels (snow and ice applications, bright salt pans), from diagnostic features in the visible to near-infrared wavelength range (water, snow and ice) to longer wavelengths in the short-wave infrared (mineral and soil applications), from wide spectral features (vegetation, soil) to narrow-absorption features (mineral, greenhouse gases), using various state-of-the-art processing and analyses methodologies in imaging spectroscopy

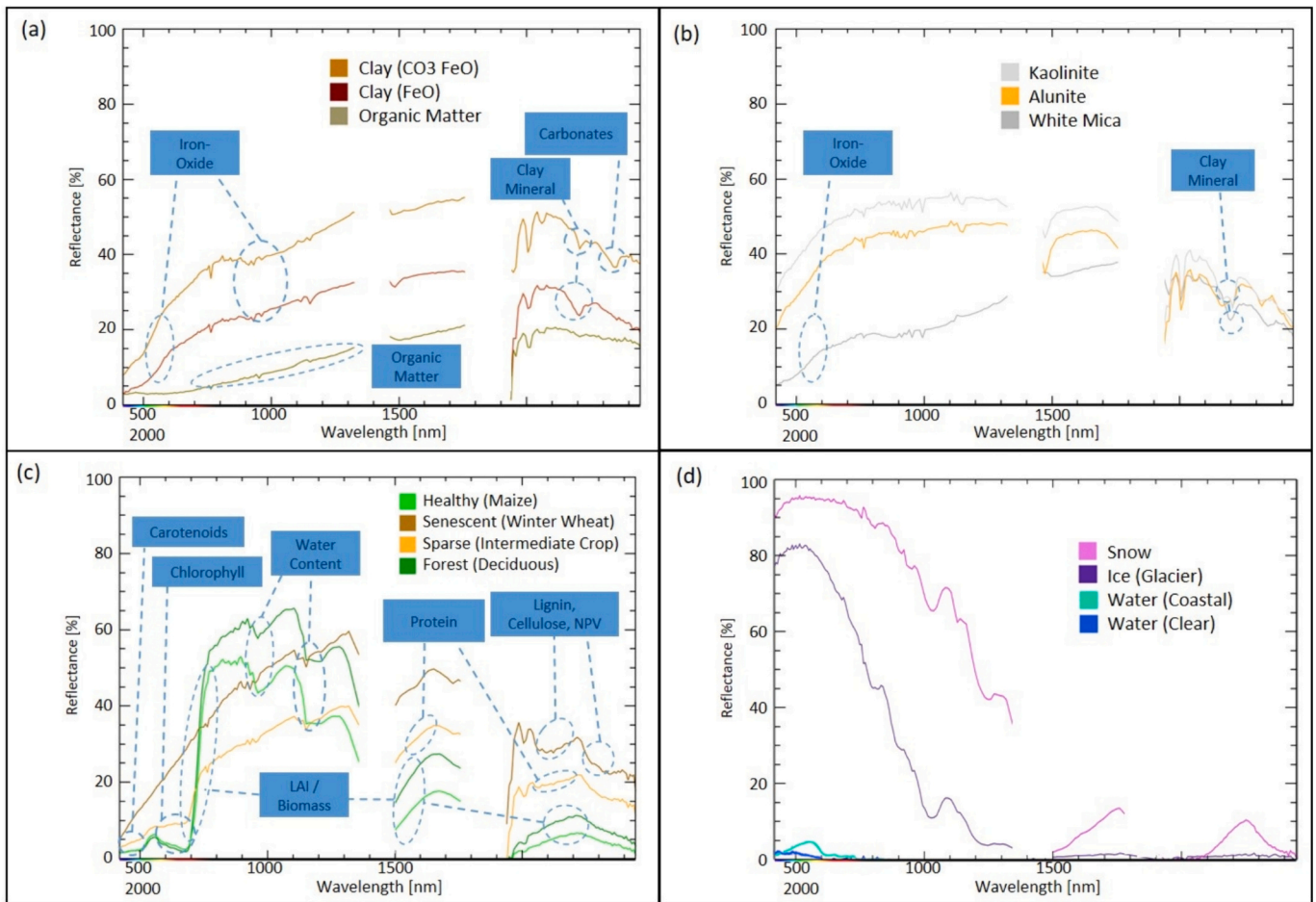


**Fig. 3.** Various exemplary reflectance spectra representing different scientific applications a) Soils, b) Minerals, c) Vegetation, and d) snow, ice and water. Important characteristic features of interest are highlighted with circles. The spectra were extracted directly from original EnMAP L2A products without applying any polishing or smoothing.

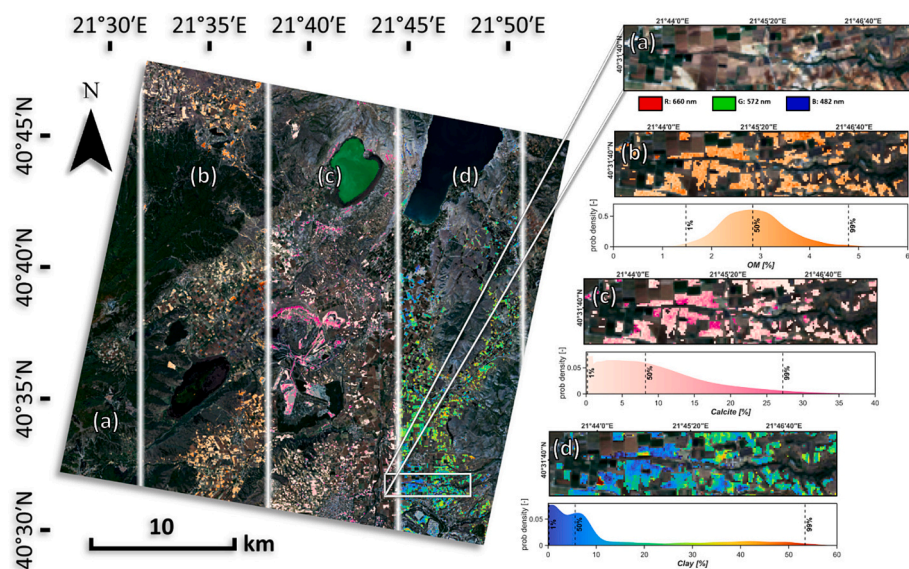


**Fig. 4.** Composite of quantitative soil property maps estimated with GPR based on the central region of two successive EnMAP scenes acquired on 7 October 2022 and field data collected in 2018-2019 over an agricultural area located in the West Macedonia Region, in Northern Greece: Left: Composite map and Right: Subset (a) true-color EnMAP imagery; (b) Organic Matter; (c) Calcite content; (d) Clay content. The subset images demonstrate EnMAP’s capability of resolving in-field heterogeneity. The histograms indicating the distribution of values, the color scaling, along with relevant percentiles apply to the zoom subsets.

**Table 4**

Cross-validation accuracies of soil property prediction derived from EnMAP imagery with GPR. N: Number of samples;  $R^2$ : Squared correlation coefficient; RMSE: Root-Mean-Squared Error; RPD: Ratio of performance to deviation; RPIQ: Ratio of performance to interquartile distance; MAE: Mean absolute error; nRMSE: Normalized Root-Mean-Squared Error.

Soil property	n	$R^2$	RMSE	RPD	RPIQ	MAE	nRMSE
OM	16	0.89	0.45%	3.10	0.48	0.32%	0.10
Calcite	8	0.99	1.09%	13.29	19.47	0.94%	0.03
Clay	16	0.79	7.93%	2.08	3.47	5.38%	0.17

science including spectral band convolution, radiative transfer modeling, hybrid deep learning, and machine learning. In order to facilitate result regeneration for product harmonization in future global imaging spectroscopy missions, the full scene IDs of the EnMAP products used in the examples are provided in supplementary materials (Appendix C).

#### 4.1. Soil mapping and monitoring

Soils are essential for ecosystem functioning and their extremely variable physical and chemical composition make hyperspectral data an essential tool to classify soils as well as to assess soil carbon storage, soil moisture, degradation, and contamination. The spectral reflectance characteristics of soils are mainly influenced by organic matter, clay mineral content, iron oxides, moisture, salinity, and texture representing key variables for soil health and soil quality. They represent important topics for the regular global mapping and monitoring of soil resources for which there is a high demand (Directorate-General for Environment, 2023; European Commission, Soil strategy for 2030). Well-known reflectance characteristics of soils and the use of imaging spectroscopy for soil properties mapping have been the topics of multiple scientific investigations (e.g. Ben-Dor et al., 2018; Demattè et al., 2015; Van Wesemael and Chabrillat, 2023). High-quality hyperspectral data provided by EnMAP has considerable potential to characterize the topsoil properties by quantifying soil compositional information, and their changes over time (Chabrillat et al., 2019), as well as the relationships between soil degradation and canopy spectroscopy (Milewski et al., 2022).

To showcase the potential of EnMAP imagery for soil mapping, we trained state-of-the-art machine learning models on collected soil reference information to produce quantitative predictions of three important soil properties based on EnMAP Level 2A imagery (Fig. 4). Different regression techniques (Partial Least-Square, Random Forest, Support Vector Machine, and Gaussian processing) and spectral pre-treatments of EnMAP reflectance data (e.g., absorbance transformation, normalization, first and second derivative) were tested and their optimal hyperparameters were selected using Bayesian optimization in 120 iterations in 5-fold cross-validation. Here, Gaussian Process Regression (GPR) (Rasmussen and Williams, 2006) produced the most successful models using the rational quadratic (for organic matter and calcite content) and squared exponential (for clay content) kernel functions coupled with Automatic Relevance Determination (ARD) of the spectral variables. Fig. 4 shows the derived soil maps based on two consecutive EnMAP tiles ( $30 \times 60$  km area) acquired on 7 October 2022. The soils of the region are highly diverse, originating from Triassic-Jurassic limestones, tertiary and quaternary clays, lignite, and marl-rich sediments, that form organic-rich alluvial planes (Kyriou and Nikolakopoulos, 2020). The EnMAP-based GPR models demonstrate exceptional accuracy in leave-one-out cross-validation with the locally collected soil dataset, achieving  $R^2$  of 0.89, 0.99, and 0.79 for the prediction of organic matter, calcite, and clay content, respectively (Table 4).

#### 4.2. Raw materials and mining

To meet the ever-growing global demand for non-renewable raw material resources, it is imperative to actively search for new resources and leverage the potential of re-mining tailings and waste rocks (West, 2020). Achieving these goals requires the utilization of advanced exploration tools and techniques aimed at improving the current rate of economic deposit discovery. Many economically important mineral resources are associated with alteration mineral assemblages, where one or more minerals typically exhibit diagnostic absorption features in the VNIR and/or SWIR wavelengths. Various spectral processing techniques enable the direct extraction of mineralogical information in the form of abundance, composition, crystallinity, and classification maps (Asadzadeh and de Souza Filho, 2016). The abundance maps can provide semi-quantitative information about the proportion of minerals within each pixel. The compositional maps, on the other hand, can reveal the chemistry of specific minerals and thereby elucidate the physiochemical conditions (T, P, pH, redox, and chemical activities) of the mineralized system(s) providing vectors towards the zones of metal deposition (Cudahy et al., 2008). An example of a compositional mineral map is shown in Fig. 5, where the accurate position of the 2200 nm white mica absorption feature, determined by fitting a 2nd-order polynomial to the apparent minimum and its two neighboring bands in continuum removed spectra, is used to reveal variations in the mineral chemistry and point towards the core center of mineralization for further exploitation targets (blue areas). In this example, the core center of mineralization points towards current or old tailings and new areas have not yet been exploited, and such maps as provided by EnMAP are upon further validation of extremely high interest. The methods and algorithms used in this example have been already exploited and successfully validated based on airborne imaging spectroscopy (Asadzadeh et al., 2023), facilitating the confidence in the EnMAP map obtained. In addition, mineral maps can reveal clear indicator minerals to identify surface expressions of mineralisations as by detection of iron oxides/iron hydroxides, as demonstrated already by Schodlok et al. (2022).

This example shows that by being able to accurately resolve narrow VNIR and SWIR mineral spectral features, EnMAP can offer a rapid and cost-effective tool for mapping surface mineralogy over geological outcrops and mining sites. In particular, the high SNR in the SWIR and accurate spectral calibration are essential for surface mineral mapping. Overall, the EnMAP well-calibrated, high spectral resolution data enable the detection of a wide range of spectrally active minerals including hydroxyl-bearing silicates, sulphates, carbonates, borates, ammonium-bearing minerals, iron oxides/hydroxides, and potentially rare earth elements (REE) (Chabrillat et al., 2022). While the utilization of spectral remote sensing data has reached maturity for certain ore deposits like porphyry copper and epithermal gold deposits, the application of this technology is still considered immature or at best semi-mature for other deposit types particularly for some critical minerals such as lithium and REEs. This highlights the importance of conducting more case studies using the EnMAP hyperspectral data. Such studies can make substantial contributions to the understanding of ore deposit formation and their surface footprints. EnMAP-based exploration will become invaluable for regional-scale mineral exploration, ore targeting, and support for exploration drilling, and re-mining of historical wastes and tailings.

#### 4.3. Vegetation

Detailed, multi-scale monitoring of vegetation patterns and processes on the land surface has far-reaching environmental, economic, and societal implications. In many studies, imaging spectroscopy has demonstrated its high suitability for quantifying key plant traits due to strong absorption and reflectance features across the VNIR-SWIR spectrum indicating foliar pigments, leaf and canopy structure, as well as nitrogen-containing compounds, lignin and cellulose (Ollinger, 2011). Imaging spectroscopy can measure vegetation properties such as

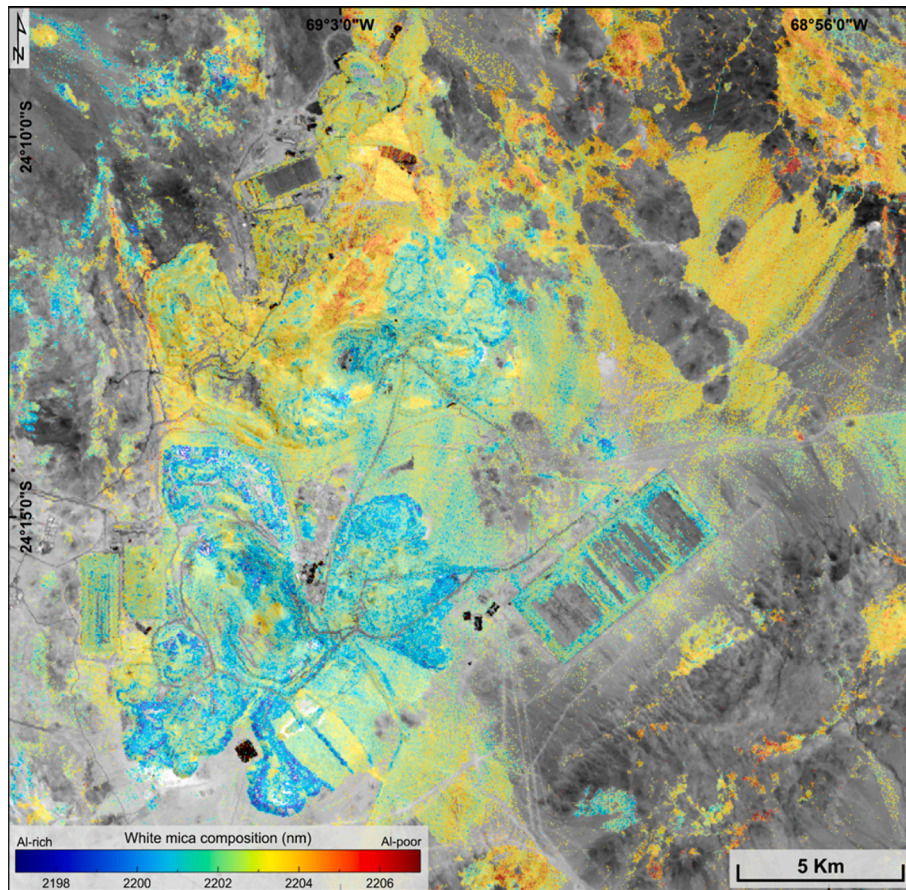


**Fig. 5.** Variations in the composition of white mica across the Escondida mining area (Chile) revealed by EnMAP hyperspectral data from 07 March 2023. The absorption minimum of white mica around 2200 nm shifts towards shorter wavelengths, indicating Al-rich mineral chemistry towards the mineralized centers (now copper mines). In this sense, it provides a vector for prospecting similar deposits in arid to semi-arid regions of the world.

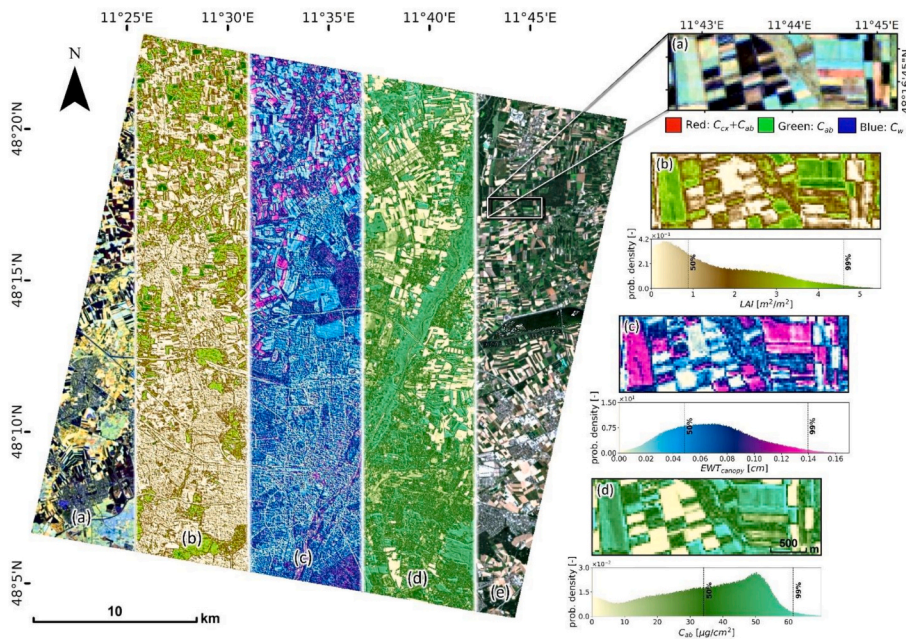


**Fig. 6.** Composite of a full EnMAP-scene ( $30 \text{ km} \times 30 \text{ km}$ ) from Southern Germany (28 July 2022) consisting, from left to right, of an RGB-blend of carotenoids, chlorophyll and liquid water absorption integrals (a), quantitative maps of leaf area index (b), canopy water content (c) and leaf chlorophyll content (d), as well as a true-color image (e). The zoom images on the right demonstrate EnMAP's capability of resolving in-field heterogeneity that is relevant for site-specific management. The histograms indicating the distribution of values along with minimum, maximum, and average apply to the full extent of the image.

**Table 5**  
PROSAIL Variables.

Symbol	Variable Name	Unit	Lower Bound	Upper Bound
N	Leaf Structure Parameter	–	0.7	4
Cab	Chlorophyll a + b Content	$\mu\text{g}/\text{cm}^2$	0	150
Cxc	Carotenoid Content	$\mu\text{g}/\text{cm}^2$	1	50
Anth	Anthocyanin Content	$\text{nmol}/\text{cm}^2$	0	15
Cbrown	Brown Pigments Content	arbitrary units	0	1
Cw	Leaf Water Content	$\text{g}/\text{cm}^2$	0.0002	0.1
Prot	Protein Content	$\text{g}/\text{cm}^2$	0.0001	0.03
CBC	Carbon-based constituents Content	$\text{g}/\text{cm}^2$	0.001	0.06
ALIA	Average Leaf Inclination Angle	$^\circ$	40	50
LAI	Leaf Area Index	$\text{m}^2/\text{m}^2$	0.5	15
Drysoil	Fraction of Dry Soil	–	0	1

vegetation composition, structure, plant functional traits, and plant vitality, which in turn indicate ecosystem composition, functioning, and early recognition of environmental stress (Cherif et al., 2023; Cooper et al., 2021; Feilhauer et al., 2018, 2021; Zhang et al., 2021). Previous studies based on simulated EnMAP data have been successfully carried out for a diverse selection of managed and natural ecosystems including croplands (Locherer et al., 2015; Berger et al., 2018a; Danner et al., 2021), wetlands (Gasela et al., 2022), shrublands (Schwieder et al., 2014; Suess et al., 2015), wildland-urban interface (Cooper et al., 2020; Jänicke et al., 2020; Okujeni et al., 2021), subalpine and alpine ecosystems (Jędrych et al., 2017; Marcinkowska-Ochtyra et al., 2017), and Arctic tundra (Beamish et al., 2017). EnMAP data will be key to describing the spatial and temporal variability of plant traits at scales relevant for comprehensive monitoring as well as Earth system and ecosystem modeling (Cherif et al., 2023; Rogers et al., 2017; Zhang et al., 2021). Additionally, EnMAP data will facilitate the derivation of Essential Biodiversity Variables (EBV) at regional scales (Pereira et al., 2013; Skidmore et al., 2015, 2021) and improve carbon emission monitoring and accounting (Numata et al., 2011; Nurda et al., 2020) both being crucial to achieving targets set by the European Green Deal. Below two studies on agricultural and forest applications are showcased demonstrating that high-quality spaceborne EnMAP data are equally suitable as previously acquired airborne hyperspectral data for deriving key plant properties and thus will allow to be used for future ecosystem monitoring.

#### 4.3.1. Agriculture

Potential applications of hyperspectral remote sensing for agricultural purposes are numerous (Hank et al., 2019) and knowledge about the dynamics of plant traits in space and time is highly relevant for information-driven, engineered, site-specific crop production. Fig. 6 shows a composite of a full EnMAP Level 2A scene (30 km  $\times$  30 km) from an agricultural site in Germany – the Munich-North-Isar (MNI) test site (Danner et al., 2017; Woche et al., 2018). While Fig. 6e displays a true-color image using EnMAP bands at 482, 572 and 660 nm, Fig. 6a shows an RGB-blend of carotenoids, chlorophyll and liquid water absorption integrals derived via the continuum-removed integral calculation from the Analyze Spectral Integral tool (Woche et al., 2020), which represents a parametric method (see also Table A.1). The quantification of canopy water content in Fig. 6c is based on the iterative inversion of the Beer-Lambert law and thus represents a physically-based approach (Woche et al., 2018). The quantitative maps of leaf area index (LAI) and leaf chlorophyll content (Fig. 6b and d) were achieved by training an artificial neural network with simulated RTM data and are examples of hybrid retrievals (Woche et al., 2022). The MNI test site is characterized

by intensive crop production, with predominantly cultivated cereals and maize. The analyses demonstrate the capability of EnMAP to deliver spatial information products with relevance for practical precision farming. Structural information, such as quantitative LAI, for example, are needed for yield estimation and crop protection measures, while chemical information, e.g. pigment concentration and water status, are relevant for decisions on crop health and nutrition supply management. In this first example, no in-situ data could be made available at the time of the overpass and a quantitative validation will be needed in the future which will take place based on regular field campaigns at EnMAP overpasses. Nevertheless, the histograms for the different biophysical and biochemical variables reveal that absolute values as well as distributions of the retrieved quantitative information are realistic, although no in-situ data was used for calibration of the retrieval algorithms. The EnMAP observation exemplarily shown in Fig. 6 took place towards the later stages of the crop's phenological cycle. At this time, the cereal fields had either been harvested or were in a highly advanced stage of senescence. The remaining green fields primarily consisted of silage maize, which is characterized by significant values of LAI and elevated levels of chlorophyll and water contents. In addition to green variable retrievals, it is to be expected that EnMAP data will contribute significantly to the estimation of non-photosynthetic vegetation in the upcoming years (Verrelst et al., 2023).

#### 4.3.2. Forest

The vast areas covered by forests demand remote observations to determine parameters like tree species distribution, forest health, and forest productivity. While many parameters of interest are routinely measured using multispectral satellites, some are only accessible with hyperspectral data, e.g., non-chlorophyll pigments like carotenoids (Fassnacht et al., 2015; Sonobe and Wang, 2018) and anthocyanins (Féret et al., 2017; Gitelson et al., 2006), protein and nitrogen concentrations (Schlerf et al., 2010; Wang et al., 2018), and the current level of photosynthesis that can be estimated using the photochemical reflectance index (PRI) (Gamon et al., 1997). In Fig. 8 we show a forest trait mapping example focusing on a mostly cloud-free EnMAP Level 2A composite of the Hunsrück-Hochwald National Park (NPHH) in western Germany acquired on 28 June 2022 (western part) and 17 July 2022 (eastern part). The NPHH is Germany's youngest national park and was established in 2015. The forest is dominated by Norway spruce (*Picea abies*), beech (*Fagus sylvatica*), sessile oak (*Quercus petraea*), and Douglas fir (*Pseudotsuga menziesii*). The spruce trees in particular have been under severe drought stress and were subsequently attacked by bark beetles that resulted in massive die offs. In order to map leaf and stand traits, the PROSAIL canopy reflectance model (Jacquemoud et al., 2009)

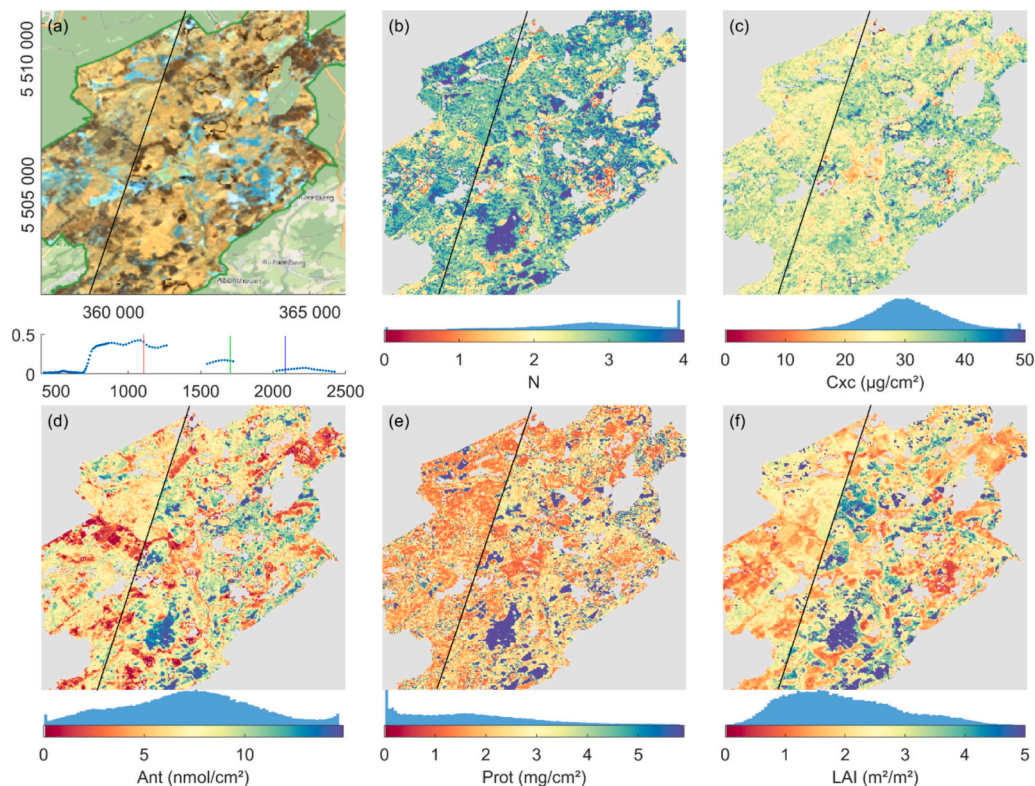


**Fig. 7.** Forest trait mapping based on a subset of EnMAP images of the southwestern part of National Park Hunsrück-Hochwald forest in Germany based on PROSAIL inversion: a) false-color composite of shortwave infrared bands (red = 1110 nm, green = 1715 nm, blue = 2070 nm, with the bands marked by vertical lines in the spectrum below the first panel), b) Nitrogen, c) Total Carotenoid content, d) Antocyanins, e) Proteins, and f) LAI PROSAIL parameters. A black line separates scenes of 28 June (Western part) and 17 July 2022 (Eastern part). (For interpretation of the references to color in this figure legend, the reader is referred to the web version of this article.)

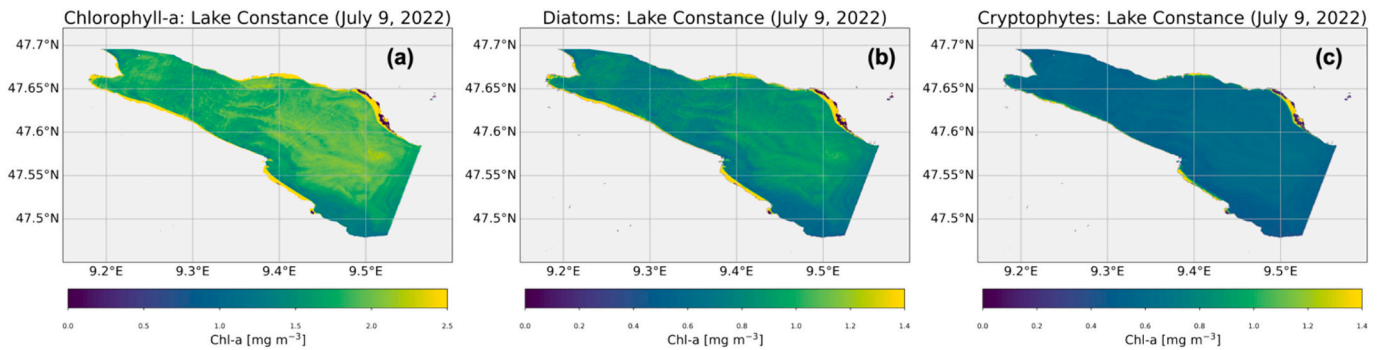
was inverted. We combined PROSPECT-Pro (Féret et al., 2021), the latest version of the PROSPECT leaf radiative transfer model (Jacquemoud and Baret, 1990), with 4SAIL (Verhoef et al., 2007). With PROSPECT-Pro, different classes of pigments (chlorophylls, carotenoids, and anthocyanins) as well as proteins and non-protein dry matter, can be mapped at the same time. Inversion was performed using the trust-region reflective algorithm (Jay et al., 2016). Free parameters and their bounds used for the inversion are listed in Table 5.

Fig. 7 shows the results of the inversion process for some selected parameters. For each parameter, a histogram is shown. Most retrieved values are in plausible ranges of values, but N values are unexpectedly high with some pixels saturated at  $N = 4$ . The spatial patterns reveal stands of different species, ages, and health. The LAI inversion shows the difference between the June and July captures and points out to affected areas. Differences between the Western and Eastern parts of the image are most obvious for the Protein content and LAI, and probably show phenological forest development during the dynamic early summer phase. Although for this example no field campaign could be planned during the commissioning phase to validate the results, such algorithms and methods were largely validated based on airborne imaging spectroscopy (e.g. Hill et al., 2019), and further field campaigns will improve confidence in the results.

#### 4.4. Inland and coastal waters

Water quality of inland and coastal waters has important implications for habitat quality, food supply, commerce and human health, and

recreation. Dissolved and particulate materials in addition to water molecules interact with the underwater light by absorption and scattering. These optical constituents such as chlorophyll, phytoplankton functional types, dissolved organic matter, and suspended sediments being variable in time and space can be mapped by multispectral and hyperspectral remote sensing (Bracher et al., 2021; Brando and Dekker, 2003; Bresciani et al., 2022; Giardino et al., 2019; Hestir et al., 2015; Lima et al., 2023; Niroumand-Jadidi et al., 2020). The main advantage of imaging spectroscopy is that spectral differences in the inherent optical properties of the water bodies can be better captured by hyperspectral sensors due to their higher spectral resolution. In the result, improved estimates of the composition of organic matter can be achieved. The quantification of these constituents can in turn contribute to the understanding of diverse processes such as carbon cycling, nutrient availability, coastal and inland water management, as well as endangered ecosystems (coral reefs, seagrass meadows, and mangrove forests). Particularly, the quantification of phytoplankton functional types represents important proxies for ecosystem functioning (Bracher et al., 2017, 2022). Indeed, specific phytoplankton types can grow rapidly, build up very large biomass or even produce toxins, and by that become harmful to the environment in the form of so-called harmful algal blooms (HABs). In this context, we present for the first time EnMAP retrievals of phytoplankton functional types. The study area is Lake Constance; the second largest lake in Europe, located on the north-western edge of the Alps and used as a drinking water reservoir for about 5 million people (Petri, 2006). The lake covers approximately 535 km<sup>2</sup> with a volume of 48.4 km<sup>3</sup> and a maximum depth of 252 m (Petri,



**Fig. 8.** Spatial distribution of water properties based on EnMAP L1B image at Lake Constance retrieved with POLYMER Atmospheric Correction using the EnMAP-Box-EnPT-Acwater-Polymer tool and with the EnMAP-Box OC-PFT tool: a) chlorophyll-a concentration (mg/m<sup>3</sup>), b) diatom Chl-a concentration (mg/m<sup>3</sup>), and c) cryptophytes Chl-a concentration (mg/m<sup>3</sup>).

2006). The trophic status of the lake is characterized as oligotrophic following a period of severe eutrophication in the 1960s and 1970s (Murphy et al., 2018). Snowmelt and precipitation are the main drivers of the lake's water level (Petri, 2006).

In July and August 2022, Lake Constance (Germany) experienced water levels close to the lowest records ever observed which were caused by an extended period of drought and high temperatures that triggered high phytoplankton pigments concentrations (IGKB, 2024). To get an overview of these extensive growths, we retrieved the concentration of phytoplankton functional types at Lake Constance on 9 July 2022 based on EnMAP Level 1B product, processed to Level 2A using the

EnMAP-Box-EnPT tool and choosing the POLYMER atmospheric correction (Soppa et al., 2021; Steinmetz et al., 2011; <https://www.hygeos.com/>) to retrieve normalized water-leaving reflectance as well as several additional products such as chlorophyll-a concentration (Chl-a). The EnMAP Chl-a product (Fig. 8a) was then used as input data in the OC-PFT tool implemented in the EnMAP-Box (See Table A.1). The retrievals show that diatoms were the dominant phytoplankton type on 9 July 2022, followed by cryptophytes (Fig. 8b,c). In comparison to in-situ data, the concentrations of the EnMAP-based total Chl-a and Diatoms-Chl-a are in the expected range, although the total Chl-a and diatoms Chl-a are underestimated. The median EnMAP diatom-Chl-a was 0.82

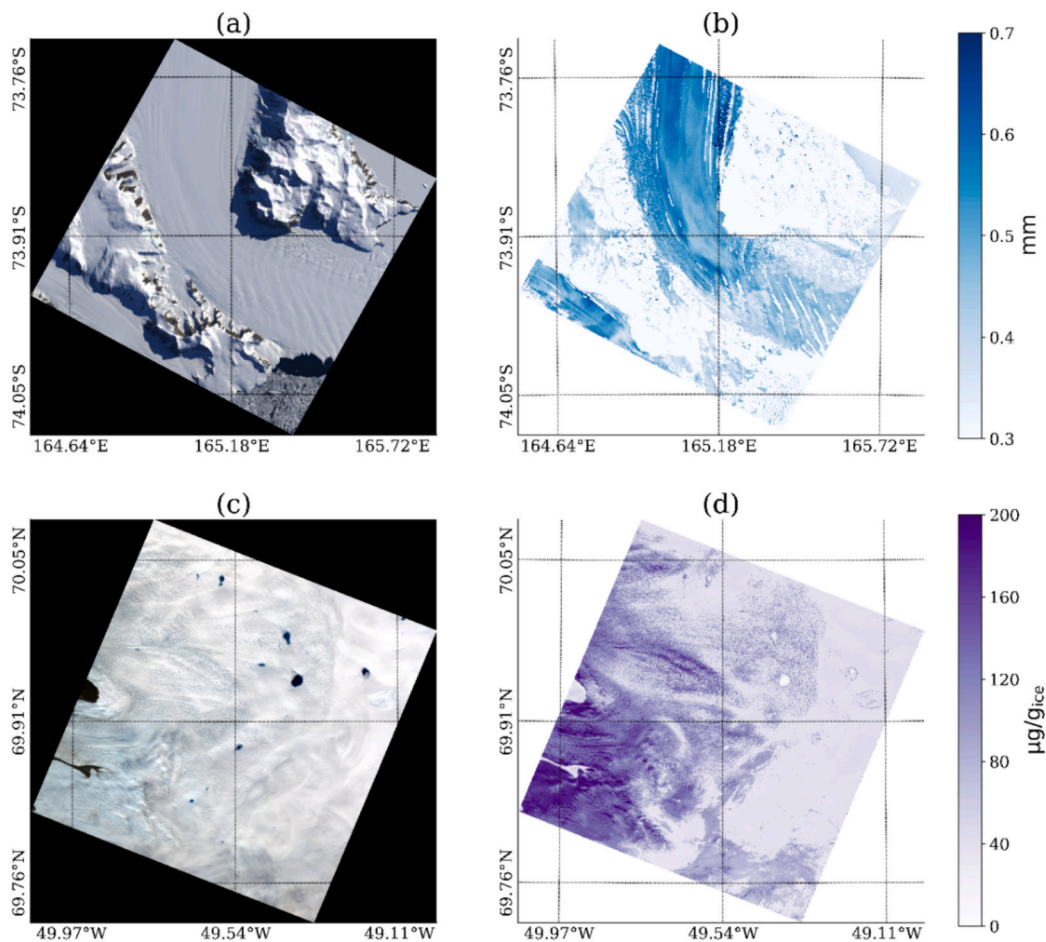


**Fig. 9.** Snow surface properties derived from EnMAP imagery: a) Aviator Glacier in Antarctica (TrueColor RGB, 16 February 2023), b) Snow grain size retrieved in mm, c) south-west coast of Greenland (TrueColor RGB, 1 September 2022), d) Algae concentration retrieved in µg/g<sub>ice</sub>

mg/m<sup>3</sup>, in contrast to the corresponding median derived from in-situ measurements of 1.31 mg/m<sup>3</sup>. Both EnMAP and in-situ exhibited a median value of 0.58 mg/m<sup>3</sup> for cryptophytes-Chl-a.

#### 4.5. Cryosphere

The cryosphere includes snow, sea ice, lake and river ice, icebergs, glaciers and ice caps, ice sheets, ice shelves, permafrost, and seasonally frozen ground (World Meteorological Organization WMO). Global-scale glacier mass loss, permafrost thaw, and decline in snow cover and Arctic sea ice extent are projected to continue in the near term. Human communities in close connection to coastal environments, polar areas, and high mountains, are particularly exposed to ocean and cryosphere change (IPCC, 2022).

Rapid warming, impurity-darkening and darkening due to the loss of sea ice in the ocean and the densification of high vegetation on the land surface of the cryosphere induce a wide range of complex feedback mechanisms that have cascading hydrological, geomorphological, climatic, and ecological effects (Post et al., 2009; Prev y et al., 2017; Sarangi et al., 2020; Skiles et al., 2018; Wrona et al., 2016). Despite having limitations due to polar night and high cloud cover in summer, optical remote sensing is a key tool for monitoring remote and complex cryosphere systems and tracking their changes in the perturbed climate system. In particular, hyperspectral remote sensing offers the required accurate quantification of snow and ice surface properties, which in turn can improve our understanding of feedback mechanisms as well as energy, water, sediment, and carbon fluxes (National Academies of Sciences, Engineering, and Medicine, 2018; Painter et al., 2013). The main properties of interest include snow grain size and impurity concentration, whose subtle absorption features can be resolved by hyperspectral data. Ice is most distinctively absorptive in the NIR around 1030 nm, while impurities lower the albedo in the VIS between 400 and 700 nm.

In this example, two EnMAP snow processing algorithms have been applied to EnMAP L1C polar acquisitions from two different locations: the analytical solution of the inverse snow optics problem based on the asymptotic radiative transfer (ART) is applied to a scene from Antarctica to retrieve grain size (Kokhanovsky et al., 2023a, 2023b), while the Optimal Estimation (OE) based on simultaneous atmosphere and surface modeling is used to infer glacier algae concentration from the Greenland Ice Sheet (Bohn et al., 2021, 2022). Fig. 9b presents snow grain size from the ART framework. An in-depth validation and extension to retrieve total ozone and water vapor columns over snow is performed by Kokhanovsky et al. (2023b). Fig. 9d shows the derived concentration of glacier algae at the Southwest coast of Greenland in late Summer 2022. Impacted by the annual melting season, broad colonies of algae cells have accumulated on the surface, particularly in the so-called ‘dark

zone’ at lower altitudes with closer proximity to the shoreline.

#### 4.6. Anthropogenic greenhouse gas emissions

Detecting, quantifying, and mitigating greenhouse gas emissions from anthropogenic sources is crucial to slowing climate change. Though not designed as atmospheric instruments, imaging spectrometers are well suited to retrieving concentrations of methane, carbon dioxide, and water vapor given the absorption of these gases in the NIR and SWIR spectral regions. This was first demonstrated using the AVIRIS-NG airborne spectrometer (Roberts et al., 2010; Bradley et al., 2011; Thorpe et al., 2017), and more recently for the satellite case using first Hyperion (Thompson et al., 2016) and then PRISMA (Guanter et al., 2021) for methane and in Cusworth et al. (2021) for carbon dioxide.

In particular, spaceborne imaging spectrometers are being extensively used for the detection of methane emissions from the fossil fuel industry. These emissions often happen as plumes of highly concentrated gas, emitted from so-called point sources, which are relatively small infrastructure elements such as valves or vents. The methane absorption band in 2100-2450 nm can be used to generate maps of methane concentration enhancements, that is, anomalies in methane concentrations with respect to the background concentration levels. These maps are exploited to detect and quantify methane plumes, and also to attempt the attribution of the plumes to potential sources in the area.

In this example, large methane plumes are mapped with EnMAP as shown in Fig. 10. The methane plumes were derived from EnMAP top-of-atmosphere radiance data acquired over oil and gas extraction infrastructure in Turkmenistan on 6 October 2022, using the methods described in Roger et al. (2024). In short, a per-pixel methane concentration enhancement is estimated using a retrieval method based on the matched-filter principle (Thompson et al., 2016). Four strong methane concentration enhancements are visible within the imaged area. The performance of EnMAP to map methane plumes is discussed by Roger et al. (2024), which show the smaller methane retrieval errors for EnMAP with respect to PRISMA due to EnMAP’s higher spectral resolution and signal-to-noise ratio in the SWIR. In this regard, the potential of EnMAP to retrieve low methane emissions due to its high data quality is essential and will need to be proved in the future.

#### 4.7. Natural and anthropogenic hazards

EnMAP data overall will improve identification and monitoring of both natural and man-made hazards as well as vulnerability and risk, including landslides, swelling clays, flood and drought impacts, volcanoes, land degradation and soil erosion, contamination, and oil spills.

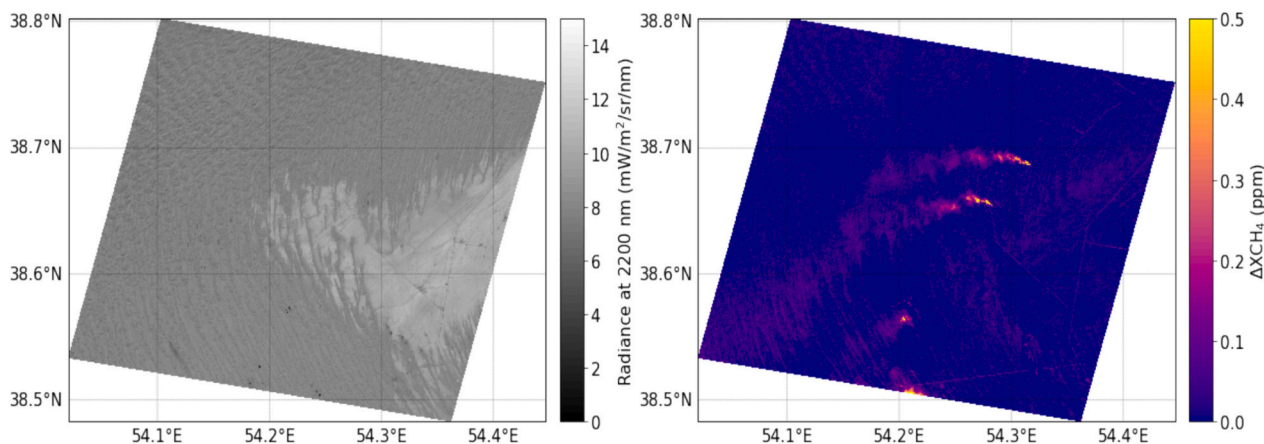


**Fig. 10.** Maps of at-sensor radiance at 2200 nm and methane concentration enhancement ( $\Delta XCH_4$ ) derived from an EnMAP L1B dataset (top-of-atmosphere radiance) acquired over an oil and gas extraction basin on the west coast of Turkmenistan on 6 October 2022.

Overall, the main benefit of hyperspectral data lies in their potential for a more detailed, material-oriented characterization of factors and impacts contributing to hazards. For example, imaging spectroscopy can further improve the characterization of the driving factors of landslides and other hazards. This includes a better characterization of lithological conditions and improved identification of inhomogeneities within landslide-prone slopes, which indicate increased potential for the onset of slope failures. It can also improve the characterization of landslide deposits including their revegetation over time. Also, expansive clays and clay-shales cause costly damages worldwide every year. Soil spectroscopy has been shown to be a useful tool for evaluating the expansive potential of soils (Goetz et al., 2001). Imaging spectroscopy, with its potential for direct identification of constituent minerals in soils, can facilitate the detection and mapping of expansive clays in different locations and at different spatial scales (Chabrillat et al., 2002). Furthermore, some recent use of EnMAP observation capabilities were used to monitor an oil spill off the coast of Brazil and the first results seem to indicate the potential to identify the thickness of such oil spills (Asadzadeh et al., Pers. Com.). Another example is the use of EnMAP data after heavy rainfalls in Somalia in March-May 2023 to provide crisis information in the frame of the International Charter “Space and Major Disasters”.

Another field of new EnMAP applications is the domain of nighttime lights. As shown by Bachmann and Storch (2023), the EnMAP radiometric sensitivity and overall performance are good enough that for the first time full VNIR-SWIR nighttime spectra could be retrieved from a satellite mission. Thanks to the high signal-to-noise ratio and fine spectral resolution of EnMAP, the dominant lighting types were identified based on the spectrally resolved emission features, and also high-temperature events like fires were detected based on the short-wave infrared emissions. In combination with the total emitted light power derived from e.g., the VIIRS Day/Night Band, EnMAP can thus contribute to a better understanding of the Earth at night, and thus a better understanding of environmental impact.

Another aspect is the environmental consequences of mineral exploration and mining of minerals and other non-renewable resources. Sustainable development of these resources has been a prime focus for the last few decades. Nowadays, most developed countries have

regulations and policies in place to safeguard the environment. However, historically this has not been the case. One of the most common environmental challenges associated with mining is acid mine drainage (AMD) and the release of toxic metals into downstream watersheds posing risks to human and ecosystem health (Swayze et al., 2000). The ability of EnMAP data to characterize secondary minerals resulting from AMD processes together with the synoptic view of other orbital data represents a vast potential for the characterization, monitoring, and estimation of the risks related to such hazards. The data can be applied to address different issues including monitoring land cover changes, detecting and mapping soil erosion and vegetation loss, identifying areas susceptible to acid mine drainage and other contamination risks, monitoring and managing waste materials and tailings storage facilities, and evaluating restoration efforts such as vegetation regrowth and ecosystem recovery (Ong and Cudahy, 2014; Richter et al., 2008; Swayze et al., 2000; Zabcic et al., 2014). Additionally, this technology can be employed to quantitatively map mineral-derived dust from the transportation and handling of mineral resources (Ong et al., 2003). This example exploited a combination of the diagnostic capability of spectroscopy to detect and quantify iron oxides on top of identifying green vegetation, in order to quantitatively map the weight of iron oxide dust on the surfaces of mangroves (Ong, 2013). Fig. 11 demonstrates the transferability of the algorithm to EnMAP, where the relative abundances of iron ore-derived dust were derived using EnMAP data. The abundance and distribution of dust align well with previous work conducted with airborne imaging spectroscopy. That is, the highest abundances are found close to the handling facilities and iron ore stockpiles and the distribution of dust decreases away from the facilities. Further validation of the derived map will be conducted to verify the abundances and assign units ( $\text{g}/\text{m}^2$ ) to the derived maps.

These case histories demonstrate that EnMAP data in combination with high-spatial and/or high-temporal resolution multispectral datasets has the potential to become an efficient operational basis for monitoring throughout a mine’s life cycle including the characterization of the impacts of exploration and mining activities on landscape and geo-environments, as well as monitoring the progress of rehabilitated sites towards closure criteria. Tailored information products derived from spaceborne hyperspectral imaging such as EnMAP have a high

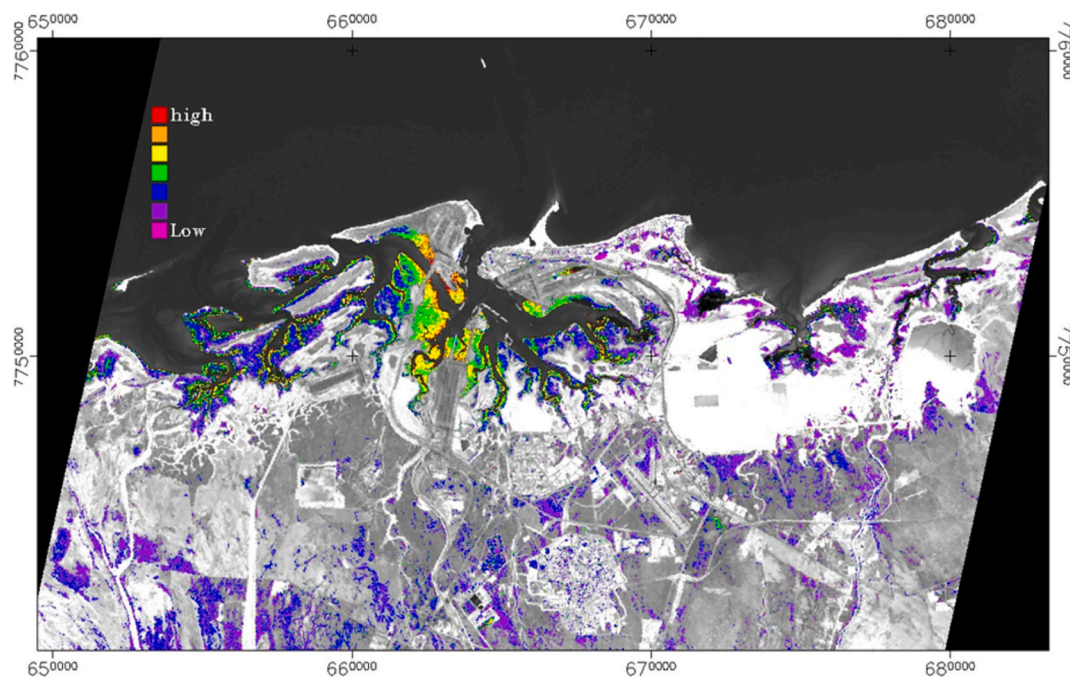


**Fig. 11.** Map of relative abundances of iron oxide dust on mangroves derived from an EnMAP L2A dataset (surface reflectance) acquired on 29 August 2023 across one of the world’s largest iron ore handling facilities in Port Hedland, Western Australia.

potential to support enhanced environmental decision-making and measures for the industry and regulatory bodies.

## 5. Synergies and prospects

In addition to the delivery of new Earth bio-and geosphere surface and atmospheric information, the role of the EnMAP science mission as a precursor for envisioned operational missions such as CHIME and SBG is widely recognized. EnMAP is a pioneering mission for global hyperspectral mappers in many respects including high-quality data due to on-board calibration, comprehensive external validation based on the support of the international science community, pointing capability, land/water/combined atmospheric correction, user-driven data acquisitions, scientific support activities including software development, educational program, end-to-end data simulation. Another strong aspect pursued by EnMAP has been the open science policy: open data access, open software, and open education that has been provided to the user community accompanied by processing and analysis tools, educational materials, calibration and validation in-situ datasets, test data for new research fields and new methodological developments. Additionally, the EnMAP mission supports the development of data harmonization and data integration across different sensors also by providing many metadata entries. In this regard, the EnMAP mission collaborates and develops synergies with current and future imaging spectroscopy missions. EnMAP's intensive international collaboration through the EnSAG, the EnMAP validation teams, and partners from the scientific exploitation program, has been leading to a strong growth of the hyperspectral community since the start of EnMAP preparations, and further intensification of international collaboration is expected with other future imaging spectroscopy Earth Observation missions already being on their way.

In this context, we expect in the next decade that global imaging spectroscopy mapping will become widely available, moving from niche to mainstream also for remote sensing users who are currently not using imaging spectroscopy yet. The expected increase in global data availability from spaceborne missions will radically change the available information on Earth surface properties and processes and allow moving from qualitative to quantitative monitoring. This in turn will cater to the need for deriving up-to-date dynamic information on Earth's surface properties for the management of resources, and support of related policies and programs. Thus, an improved understanding of the interlinkages between ecosystems and processes towards sustainable resource use and management will be supported, enabling an improved understanding of the Earth's surface processes and responses to anthropogenic and climate changes.

Though designed as a stand-alone mission, synergies of EnMAP with other spaceborne missions are essential particularly with existing optical and radar missions, and current imaging spectroscopy missions (Guanter et al., 2019). For example, the comparable spatial resolution of the Copernicus Sentinel-2 satellites (Drusch et al., 2012) to EnMAP, in combination with the higher temporal resolution and global coverage, offers promising opportunities. For instance, the combination of the temporal resolution of Sentinel-2 with EnMAP's higher spectral resolution can support improved characterization of dynamic Earth surface processes. One example is a salt pan study where one hyperspectral Hyperion image and Landsat time-series data were combined to derive a better understanding of the salt pan cycle in Namibia (Milewski et al., 2020). Further synergies are possible with very high-resolution optical data from commercial platforms such as WorldView, QuickBird, RapidEye, and Pleiades which can augment object recognition, product validation, and temporal coverage facilitating applications such as crop and forest management.

The physical surface parameters that can be derived from Synthetic Aperture Radar (SAR) such as roughness, and soil moisture, are also complementary to biogeochemical information which can be derived from EnMAP data. In soil applications, for instance, synergies between

surface roughness and moisture contents derived from SAR and the geochemical-mineralogical parameters derived from imaging spectroscopy can provide new insights for global monitoring of soil health and soil fertility. In addition to thematic synergies, digital elevation models (DEM) derived from high-resolution SAR data such as TerraSAR-X or Tandem-X can be used to correct geometric distortions in rugged terrains. Another synergy of great relevance is the fusion of hyperspectral and LiDAR data (Brell et al., 2017, 2019). The expanded spatial and spectral dimensionality provides detailed information on the small-scale interactions of irradiance and 3D surface objects, for example by combining RTM information from spectral data with structural information on 3D canopy derived from LIDAR (Kamoske et al., 2022).

Last but not least, synergies between EnMAP and other current imaging spectroscopy missions such as PRISMA, DESIS, EMIT, GF-5 and HISUI will be essential to derive denser and more global hyperspectral time-series since all of the current imaging spectroscopy missions have limited acquisition capabilities. Already some dense time series are available in selected test sites from DESIS and PRISMA, and denser time-series will be achieved by merging data from the different sensors. This will require the development of new workflows and methodologies, also for dealing with the temporal-spectral space, and it will promote new research fields and applications to emerge. We assume that imaging spectroscopy will reach sufficient maturity by 2030, and that by then the way will be open for multi-missions and multi-domain approaches based on data acquired by upcoming missions such as ESA Copernicus mission CHIME and NASA decadal mission SBG.

## 6. Conclusions

To effectively address the most pressing environmental challenges facing planet Earth, accurate, quantitative information about bio/geo/hydro/atmo-sphere is needed. The spaceborne imaging spectroscopy EnMAP mission supports this need by providing direct and indirect assessments of vegetation traits and properties, mineralogical abundance and chemistry mapping, quantitative soil compositional information, inland waters phytoplankton mapping, snow and ice properties, greenhouse gases, as well as natural and anthropogenic hazards. In this paper, we have provided an the high data quality and initial scientific application results in a wide range of disciplines, all based on EnMAP's sophisticated design, on-board calibration and advanced processing schemes. Mission summary highlights two years after launch are:

- The EnMAP mission is a target mission based on user requests, and completed with background and foreground mission.
- The mission provides well-calibrated data with high data quality performances well beyond mission requirements.
- With >2500 registered users and 565 proposals granted as of 30 June 2024, the user community shows a strong demand for EnMAP data. In areas of high demand, user requests exceed mission capacities.
- >10,700 data takes resulting in >82,000 independent image tiles of 30 × 30 km were acquired by 30 June 2024.
- EnMAP data related to various key environmental fields were analysed in the exemplary form to demonstrate their scientific potential in the fields of soil compositional mapping, raw materials identification, agricultural crop mapping, forests health, water quality, snow and ice properties, methane mapping, and natural and anthropogenic hazard.
- In all of these applications, the high signal quality of EnMAP allowed accurate quantification of bio- geo- aqua- surfaces variables and greenhouse gas properties, which are of key importance to a better understanding of terrestrial and atmospheric properties characterizing Earth surface processes related to current global challenges such as sustainable development and climate change.
- Current work within the EnMAP mission aims at maintaining the high quality and performance of the system, improving the aspect of mission capacity through additional downlink stations and

improving the acquisition strategy as well as data delivery to users by providing analyses-ready data.

In this paper, we have demonstrated initial science results for a wide range of science application fields. Thus, EnMAP can facilitate the delivery of new high-quality products for scientific observations in polar regions (snow and ice, polar vegetation), in arid and semi-arid areas (mineral mapping, soil and land degradation studies), for natural and agricultural vegetated areas (differentiation of biochemistry content, crop and forest health), for compositional soil mapping and monitoring (soil organic carbon, soil health and fertility), for coastal and inland waters quality (water bio-geochemical variables). Finally, the paper demonstrates the high potential of EnMAP for further scientific exploitation to support various geophysical and bio-geochemical fields such as key Green Deal challenges focusing on climate neutrality soil/vegetation carbon disturbances, land degradation, sustainable development goals, food security, sustainable metal sourcing.

Nevertheless, due to limitations in the EnMAP data acquisition amounting to 5000 km/day, similar to other current imaging spectroscopy missions, combined data exploitation with other satellite sensor systems is crucial in order to achieve improved spatial and temporal coverage, e.g. using S2, DESIS, PRISMA, EMIT, HISUI with the goal of global and rapid land monitoring and tracking of critical Earth System processes. Furthermore, this will allow the development of future Copernicus services, and also support the development of upcoming global operational hyperspectral missions such as CHIME and SBG through the provision of test data and algorithms. Finally, improved sustainable management of planet Earth will be supported based on global dynamic mapping and monitoring of the available resources and their changes.

#### CRediT authorship contribution statement

**Sabine Chabrillat:** Writing – review & editing, Writing – original draft, Validation, Supervision, Methodology, Investigation, Funding acquisition, Conceptualization. **Saskia Foerster:** Writing – review & editing, Writing – original draft, Funding acquisition, Conceptualization. **Karl Segl:** Writing – review & editing, Writing – original draft, Validation, Methodology, Funding acquisition, Formal analysis, Conceptualization. **Alison Beamish:** Writing – original draft, Methodology, Investigation, Conceptualization. **Maximilian Brell:** Writing – review & editing, Writing – original draft, Visualization, Validation, Software, Methodology, Data curation. **Saeid Asadzadeh:** Writing – original draft, Visualization, Software, Investigation, Data curation. **Robert Milewski:** Writing – original draft, Software, Methodology, Investigation, Data curation. **Kathrin J. Ward:** Writing – original draft, Software, Data curation. **Arlena Brosinsky:** Writing – original draft, Supervision, Formal analysis. **Katrin Koch:** Writing – original draft, Visualization, Formal analysis. **Daniel Scheffler:** Software, Methodology, Data curation. **Stephane Guillaso:** Software, Data curation. **Alexander Kokhanovsky:** Writing – original draft, Validation, Software, Methodology. **Sigrid Roessner:** Writing – review & editing, Investigation. **Luis Guanter:** Writing – review & editing, Writing – original draft, Software, Methodology, Formal analysis, Conceptualization. **Hermann Kaufmann:** Validation, Funding acquisition. **Nicole Pinnel:** Writing – review & editing, Writing – original draft, Validation, Software, Methodology, Data curation. **Emiliano Carmona:** Writing – review & editing, Writing – original draft, Supervision, Software, Data curation. **Tobias Storch:** Methodology, Formal analysis. **Tobias Hank:** Writing – original draft, Software, Methodology, Data curation. **Katja Berger:** Writing – review & editing, Writing – original draft, Methodology, Investigation. **Mathias Woche:** Validation, Methodology, Investigation. **Patrick Hostert:** Writing – review & editing, Writing – original draft, Investigation. **Sebastian van der Linden:** Writing – review & editing, Writing – original draft, Investigation, Formal analysis. **Akpona Okujeni:** Writing – review & editing, Writing – original draft,

Validation, Investigation. **Andreas Janz:** Writing – original draft, Methodology, Investigation. **Benjamin Jakimow:** Writing – review & editing, Writing – original draft, Supervision, Funding acquisition, Data curation. **Astrid Bracher:** Writing – original draft, Funding acquisition, Formal analysis. **Mariana A. Soppa:** Writing – review & editing, Writing – original draft, Visualization, Software, Data curation. **Leonardo M.A. Alvarado:** Writing – original draft, Methodology, Investigation. **Henning Buddenbaum:** Writing – review & editing, Writing – original draft, Software, Methodology, Investigation, Data curation. **Birgit Heim:** Writing – review & editing, Writing – original draft, Supervision. **Uta Heiden:** Writing – review & editing, Investigation, Data curation. **Jose Moreno:** Writing – review & editing, Writing – original draft, Investigation. **Cindy Ong:** Writing – original draft, Methodology. **Niklas Bohn:** Writing – review & editing, Writing – original draft, Validation, Software, Formal analysis, Data curation. **Robert O. Green:** Writing – original draft, Validation. **Martin Bachmann:** Writing – review & editing, Writing – original draft. **Raymond Kokaly:** Writing – review & editing, Writing – original draft, Methodology, Investigation. **Martin Schodlok:** Writing – review & editing, Writing – original draft. **Thomas H. Painter:** Writing – review & editing, Writing – original draft. **Ferran Gascon:** Writing – review & editing. **Fabrizia Buongiorno:** Writing – review & editing. **Matti Mottus:** Writing – review & editing. **Vittorio Ernesto Brandò:** Writing – review & editing. **Hannes Feilhauer:** Writing – review & editing. **Matthias Betz:** Writing – review & editing, Investigation. **Simon Baur:** Writing – review & editing, Investigation. **Rupert Feckl:** Writing – review & editing, Investigation. **Anke Schickling:** Writing – review & editing, Writing – original draft, Investigation, Funding acquisition. **Vera Krieger:** Project administration, Supervision, Writing – review & editing. **Michael Bock:** Writing – review & editing. **Laura La Porta:** Writing – review & editing. **Sebastian Fischer:** Writing – review & editing, Investigation.

#### Disclaimer

Any use of trade, firm, or product names is for descriptive purposes only and does not imply endorsement by the U.S. Government.

#### Declaration of competing interest

The authors declare that they have no known competing financial interests or personal relationships that could have appeared to influence the work reported in this paper.

#### Data availability

The authors do not have permission to share data.

#### Acknowledgments

This study was supported by the EnMAP science program (grant numbers 50EE1923 and 50EE2401) under the DLR Space Agency with resources from the German Federal Ministry of Economic Affairs and Climate Action (BMWK). A.B. and L.M.A. contributions were further supported by the TypSynSat project (grant number 50EE1915) under the DLR/BMWK funding. A portion of this research was carried out at the Jet Propulsion Laboratory, California Institute of Technology, under a contract with the National Aeronautics and Space Administration (80NM0018D0004). The authors wish to thank the ISF-LUBW for funding long-term data set phytoplankton pigments and sharing the phytoplankton HPLC dataset at Lake Constance and supporting Lake Constance campaigns, and the project “SeeWandel: Life in Lake Constance-the past, present and future”, part of the Interreg.V programme “Alpenrhein-Bodensee-Hochrhein Germany/Switzerland/Liechtenstein/Austria” funded by the ERDF and the Swiss Confederation and cantons, for financing the ship time for BS1 and HPLC data acquisition in the Bodensee in 2020. Elina Mevenkamp is gratefully

acknowledged for her support with Fig. 2c and final manuscript edition and revisions. E. Ben-Dor, N. Tziolas, and N. Tsakiridis are gratefully acknowledged for the soil campaign contributions, and P. Teiber-Siessegger and I. Dröscher for the water campaigns contributions.

## Appendix A. Supplementary data

Supplementary data to this article can be found online at <https://doi.org/10.1016/j.rse.2024.114379>.

## References

- Alonso, K., Bachmann, M., Burch, K., Carmona, E., Cerra, D., de los Reyes, R., Dietrich, D., Heiden, U., Hölderlin, A., Ickes, J., Knodt, U., Krutz, D., Lester, H., Müller, R., Pagnutti, M., Reinartz, P., Richter, R., Ryan, R., Sebastian, I., Tegler, M., 2019. Data products, quality and validation of the DLR Earth Sensing Imaging Spectrometer (DESI). *Sensors* 19, 4471. <https://doi.org/10.3390/S19204471>.
- AMAP, 2017. *Snow, Water, Ice and Permafrost in the Arctic. Summary for Policy-Makers. Arctic Monitoring and Assessment Programme (AMAP), Oslo, Norway*, 20 pp.
- Araza, A., de Bruin, S., Hein, L., Herold, M., 2023. Spatial predictions and uncertainties of forest carbon fluxes for carbon accounting. *Sci. Rep.* 13, 1–15. <https://doi.org/10.1038/s41598-023-38935-8>.
- Asadzadeh, S., de Souza Filho, C.R., 2016. A review on spectral processing methods for geological remote sensing. *Int. J. Appl. Earth Obs. Geoinf.* 47, 69–90. <https://doi.org/10.1016/j.jag.2015.12.004>.
- Asadzadeh, S., Chabrilat, S., Cudahy, T., Rashidi, B., de Souza Filho, C.R., 2023. Alteration mineral mapping of the Shadan porphyry Cu-Au deposit (Iran) using airborne imaging spectroscopic data: implications for exploration drilling. *Econ. Geol.* 119 (1), 139–160. <https://doi.org/10.5382/econgeo.5041>.
- Bachmann, M., Storch, T., 2023. First nighttime light spectra by satellite—by EnMAP. *Remote Sens.* 15, 4025. <https://doi.org/10.3390/RS15164025>.
- Bachmann, M., Alonso, K., Carmona, E., Gerasch, B., Habermeyer, M., Holzwarth, S., Krawczyk, H., Langheinrich, M., Marshall, D., Pato, M., Pinnel, N., de los Reyes, R., Schneider, M., Schwind, P., Storch, T., 2021. Analysis-ready data from hyperspectral sensors—the design of the EnMAP CARD4L-SR data product. *Remote Sens.* 13, 4536. <https://doi.org/10.3390/RS13224536>.
- Barnsley, M.J., Settle, J.J., Cutter, M.A., Lobb, D.R., Teston, F., 2004. The PROBA/CHRIS mission: a low-cost smallsat for hyperspectral multiangle observations of the earth surface and atmosphere. *IEEE Trans. Geosci. Remote Sens.* 42, 1512–1520. <https://doi.org/10.1109/TGRS.2004.827260>.
- Beamish, A., Coops, N., Chabrilat, S., Heim, B., 2017. A PHENOLOGICAL approach to spectral differentiation of low-arctic tundra vegetation communities, north slope, Alaska. *Remote Sens.* 9, 1200. <https://doi.org/10.3390/rs9111200>.
- Ben-Dor, E., Chabrilat, S., Dematte, J.A.M., 2018. Characterization of soil properties using reflectance spectroscopy. In: Thenkabail, P.S., Lyon, J.G., Huete, A. (Eds.), *Fundamentals, Sensor Systems, Spectral Libraries, and Data Mining for Vegetation*. CRC Press, pp. 187–247. <https://doi.org/10.1201/9781315164151-8>.
- Berger, K., Atzberger, C., Danner, M., Woher, M., Mauser, W., Hank, T., 2018a. Model-based optimization of spectral sampling for the retrieval of crop variables with the PROSAIL model. *Remote Sens.* 10 (12), 2063. <https://doi.org/10.3390/rs10122063>.
- Bohn, N., Painter, T.H., Thompson, D.R., Carmon, N., Susiluoto, J., Turmon, M.J., Helmlinger, M.C., Green, R.O., Cook, J.M., Guanter, L., 2021. Optimal estimation of snow and ice surface parameters from imaging spectroscopy measurements. *Remote Sens. Environ.* 264, 112613. <https://doi.org/10.1016/j.rse.2021.112613>.
- Bohn, N., Di Mauro, B., Colombo, R., Thompson, D.R., Susiluoto, J., Carmon, N., Turmon, M.J., Guanter, L., 2022. Glacier ice surface properties in south-West Greenland ice sheet: first estimates from PRISMA imaging spectroscopy data. *Eur. J. Vasc. Endovasc. Surg.* 127, e2021JG006718. <https://doi.org/10.1029/2021JG006718>.
- Bracher, A., Bouman, H.A., Brewin, R.J.W., Bricaud, A., Brotas, V., Ciotti, A.M., Clementson, L., Devred, E., Di Cicco, A., Dutkiewicz, S., Hardman-Mountford, N.J., Hickman, A.E., Hieronymi, M., Hirata, T., Losa, S.N., Mouw, C.B., Organelli, E., Raitos, D.E., Uitz, J., Vogt, M., Wolanin, A., 2017. Obtaining phytoplankton diversity from ocean color: a scientific roadmap for future development. *Front. Mar. Sci.* 4, 245888. <https://doi.org/10.3389/FMARS.2017.00055>.
- Bracher, A., Soppa, M.A., Gege, P., Losa, S.N., Silva, B., Steinmetz, F., Dröscher, I., 2021. Extension of Atmospheric Correction Polymer to Hyperspectral Sensors: Application to HICO and First Results for DESIS Data. *International Geoscience and Remote Sensing Symposium (IGARSS) 2021-July*, pp. 1237–1240. <https://doi.org/10.1109/IGARSS47720.2021.9553568>.
- Bracher, A., Brewin, R.J.W., Ciotti, A.M., Clementson, L.A., Hirata, T., Kostadinov, T.S., Mouw, C.B., Organelli, E., 2022. Applications of satellite remote sensing technology to the analysis of phytoplankton community structure on large scales. *Adv. Phytoplankton Ecol.* 217–244. <https://doi.org/10.1016/B978-0-12-822861-6.00015-7>.
- Bradley, E.S., Leifer, I., Roberts, D.A., Dennison, P.E., Washburn, L., 2011. Detection of marine methane emissions with AVIRIS band ratios. *Geophys. Res. Lett.* 38, L17072. <https://doi.org/10.1029/2011GL046729>.
- Brando, V.E., Dekker, A.G., 2003. Satellite hyperspectral remote sensing for estimating estuarine and coastal water quality. *IEEE Trans. Geosci. Remote Sens.* 41, 1378–1387. <https://doi.org/10.1109/TGRS.2003.812907>.
- Brell, M., Segl, K., Guanter, L., Bookhagen, B., 2017. Hyperspectral and lidar intensity data fusion: a framework for the rigorous correction of illumination, anisotropic effects, and cross calibration. *IEEE Trans. Geosci. Remote Sens.* 55, 2799–2810. <https://doi.org/10.1109/TGRS.2017.2654516>.
- Brell, M., Segl, K., Guanter, L., Bookhagen, B., 2019. 3D hyperspectral point cloud generation: fusing airborne laser scanning and hyperspectral imaging sensors for improved object-based information extraction. *ISPRS J. Photogramm. Remote Sens.* 149, 200–214. <https://doi.org/10.1016/j.isprsjprs.2019.01.022>.
- Brell, M., Guanter, L., Segl, K., Chabrilat, S., Scheffler, D., Soppa, M., Bohn, N., Gorrono, J., Kokhanovsky, A.L., Bracher, A., Bachmann, M., Pato, M., Schneider, M., de los Reyes, R., Langheinrich, M., Holzwarth, S., Carmona, E., Storch, T., Pinnel, N., Kokaly, R., Ong, C., Green, R.O., Moreno, J.F., Gascon, F., Hank, T., Ben-Dor, E., Di Mauro, B., Colombo, R., Milewski, R., Brede, B., Schmid, T., Anderson, C., Schickling, A., Krieger, V., Bock, M., La Porta, L., Fischer, S., 2024. Assessment of Enmap Data Quality Through Global Product Validation Activities. PREPRINT. <https://doi.org/10.2139/ssrn.4903270>.
- Brell, M., Guanter, L., Segl, K., Scheffler, D., Bohn, N., Bracher, A., Soppa, M.A., Foerster, S., Storch, T., Bachmann, M., Chabrilat, S., 2021. The EnMAP satellite-data product validation activities. In: *Workshop on Hyperspectral Image and Signal Processing, Evolution in Remote Sensing 2021-March*. <https://doi.org/10.1109/WHISPERS52202.2021.9484000>.
- Brell, M., Guanter, L., Scheffler, D., Bohn, N., Segl, K., Altenburg Soppa, M., Gorrono, J., Bracher, A., Hank, T., Bachmann, M., Carmona, E., Storch, T., Foerster, S., Schickling, A., Chabrilat, S., 2022. *EnMAP Data Product Validation - Status*.
- Brell, M., Milewski, R., Neumann, C., Ong, C., Lau, I., Hank, T., Förster, S., Chabrilat, S., 2023. *EnMAP Field Guide - In-Situ Measurements for Validation Purposes. V.1.3*, pp. 1–14. <https://doi.org/10.48440/ENMAP.2023.002>.
- Bresciani, M., Giardino, C., Fabbretto, A., Pellegrino, A., Mangano, S., Free, G., Pinardi, M., 2022. Application of new hyperspectral sensors in the remote sensing of aquatic ecosystem health: exploiting PRISMA and DESIS for four Italian Lakes. *Resources* 11, 8. <https://doi.org/10.3390/RESOURCES11020008>.
- Brewin, R.J.W., Sathyendranath, S., Kulk, G., Rio, M.H., Concha, J.A., Bell, T.G., Bracher, A., Fichot, C., Frölicher, T.L., Galí, M., Hansell, D.A., Kostadinov, T.S., Mitchell, C., Neeley, A.R., Organelli, E., Richardson, K., Rousseaux, C., Shen, F., Stramski, D., Tzortziou, M., Watson, A.J., Addey, C.I., Bellacicco, M., Bouman, H., Carroll, D., Cetinić, I., Dall’Omo, G., Frouin, R., Hauck, J., Hieronymi, M., Hu, C., Ibbello, V., Jönsson, B., Kong, C.E., Kovač, Z., Laine, M., Lauderdale, J., Lavender, S., Livanou, E., Llorc, J., Lorinczi, L., Nowicki, M., Pradisty, N.A., Parras, S., Raitos, D. E., Ruescas, A.B., Russell, J.L., Salisbury, J., Sanders, R., Shutler, J.D., Sun, X., Taboada, F.G., Tilstone, G.H., Wei, X., Woolf, D.K., 2023. Ocean carbon from space: current status and priorities for the next decade. *Earth Sci. Rev.* 240, 104386. <https://doi.org/10.1016/j.earscirev.2023.104386>.
- Celesti, M., Rast, M., Adams, J., Boccia, V., Gascon, F., Isola, C., Nieke, J., 2022. The Copernicus Hyperspectral Imaging Mission for the Environment (Chime): Status and Planning. *International Geoscience and Remote Sensing Symposium (IGARSS) 2022-July*, pp. 5011–5014. <https://doi.org/10.1109/IGARSS46834.2022.9883592>.
- Chabrilat, S., Goetz, A.F.H., Krosley, L., Olsen, H.W., 2002. Use of hyperspectral images in the identification and mapping of expansive clay soils and the role of spatial resolution. *Remote Sens. Environ.* 82, 431–445. [https://doi.org/10.1016/S0034-4257\(02\)00060-3](https://doi.org/10.1016/S0034-4257(02)00060-3).
- Chabrilat, S., Ben-Dor, E., Cierniewski, J., Gomez, C., Schmid, T., van Wesemael, B., 2019. Imaging spectroscopy for soil mapping and monitoring. *Surv. Geophys.* 40, 361–399. <https://doi.org/10.1007/S10712-019-09524-0>.
- Chabrilat, S., Guanter, L., Kaufmann, H., Foerster, S., Beamish, A., Brosinsky, A., Wulf, H., Asadzadeh, S., Bochow, M., Bohn, N., Boesche, N., Bracher, A., Brell, M., Buddenbaum, H., Cerra, D., Fischer, S., Hank, T., Heiden, U., Heim, B., Heldens, W., Hill, J., Hollstein, A., Hostert, P., Krasemann, H., LaPorta, L., Leitão, P.J., van der Linden, S., Mauser, W., Milewski, R., Mottus, M., Okujeni, A., Oppelt, N., Pinnel, N., Roessner, S., Röttgers, R., Schneiderhan, T., Schickling, A., Soppa, M., Staenz, K., Segl, K., 2022. *EnMAP science plan*. In: *EnMAP Technical Report. GFZ Data Services*, p. 88. <https://doi.org/10.48440/enmap.2022.001>.
- Cherif, E., Feilhauer, H., Berger, K., Dao, P.D., Ewald, M., Hank, T.B., He, Y., Kovach, K. R., Lu, B., Townsend, P.A., Kattenborn, T., 2023. From spectra to plant functional traits: transferable multi-trait models from heterogeneous and sparse data. *Remote Sens. Environ.* 292, 113580. <https://doi.org/10.1016/j.rse.2023.113580>.
- Clark, R.N., 1999. *Spectroscopy of rocks and minerals and principles of spectroscopy, in Manual of Remote Sensing*. John Wiley, New York, pp. 3–58.
- Cooper, S., Okujeni, A., Jánicic, C., Clark, M., van der Linden, S., Hostert, P., 2020. Disentangling fractional vegetation cover: regression-based unmixing of simulated spaceborne imaging spectroscopy data. *Remote Sens. Environ.* 246, 111856. <https://doi.org/10.1016/j.rse.2020.111856>.
- Cooper, S., Okujeni, A., Pflugmacher, D., van der Linden, S., Hostert, P., 2021. Combining simulated hyperspectral EnMAP and Landsat time series for forest aboveground biomass mapping. *Int. J. Appl. Earth Obs. Geoinf.* 98, 102307. <https://doi.org/10.1016/j.jag.2021.102307>.
- Cudahy, T., Jones, M., Thomas, M., Laukamp, C., Caccetta, M., Hewson, R., Rodger, A., Verral, M., 2008. Next generation mineral mapping: Queensland airborne HyMap and satellite ASTER surveys 2006–2008. In: *Commonwealth Scientific and Industrial Research Organization Report*, 2008. <https://doi.org/10.13140/RG.2.1.2828.1844>.
- Cusworth, D.H., Duren, R.M., Thorpe, A.K., Eastwood, M.L., Green, R.O., Dennison, P.E., Frankenberg, C., Heckler, J.W., Asner, G.P., Miller, C.E., 2021. Quantifying global power plant carbon dioxide emissions with imaging spectroscopy. *AGU Adv.* 2, e2020AV000350. <https://doi.org/10.1029/2020AV000350>.
- Danner, M., Berger, K., Woher, M., Mauser, W., Hank, T., 2017. Retrieval of biophysical crop variables from multi-angular canopy spectroscopy. *Remote Sens.* 9, 726. <https://doi.org/10.3390/RS9070726>.

- Danner, M., Berger, K., Woche, M., Mauser, W., Hank, T., 2021. Efficient RTM-based training of machine learning regression algorithms to quantify biophysical & biochemical traits of agricultural crops. *ISPRS J. Photogramm. Remote Sens.* 173, 278–296. <https://doi.org/10.1016/j.isprsjprs.2021.01.017>.
- de Lima, T.M.A., Giardino, C., Bresciani, M., Barbosa, C.C.F., Fabbretto, A., Pellegrino, A., Begliomini, F.N., 2023. Assessment of estimated phyocyanin and chlorophyll-a concentration from PRISMA and OLCI in Brazilian inland waters: a comparison between semi-analytical and machine learning algorithms. *Remote Sens.* 15, 1299. <https://doi.org/10.3390/RS15051299>.
- Demattè, J.A.M., Morgan, C.L.S., Chabrilat, S., Rizzo, R., Franceschini, M.H.D., Terra, F., Das, Vasques, G.M., Wetterlind, J., 2015. Spectral sensing from ground to space in soil science: State of the art, applications, potential, and perspectives. In: *Thenkabail, P.S. (Ed.), Remote Sensing Handbook - Three Volume Set: Land Resources Monitoring, Modeling, and Mapping with Remote Sensing*. CRC Press. <https://doi.org/10.1201/B19355-93>.
- Directorate-General for Environment, 2023. Proposal for a Directive on Soil Monitoring and Resilience - European Commission [WWW Document]. URL <https://environment.ec.europa.eu/publications/proposal-directive-soil-monitoring-and-resilience> (accessed 1.26.24).
- Drusch, M., Del Bello, U., Carlier, S., Colin, O., Fernandez, V., Gascon, F., Hoersch, B., Isola, C., Laberinti, P., Martimort, P., Meygret, A., Spoto, F., Sy, O., Marchese, F., Bargellini, P., 2012. Sentinel-2: ESA's optical high-resolution mission for GMES operational services. *Remote Sens. Environ.* 120, 25–36. <https://doi.org/10.1016/j.rse.2011.11.026>.
- Duncan, B.N., Ott, L.E., Abshire, J.B., Brucker, L., Carroll, M.L., Carton, J., Comiso, J.C., Dinnat, E.P., Forbes, B.C., Gonsamo, A., Gregg, W.W., Hall, D.K., Jalongo, I., Jandt, R., Kahn, R.A., Karpechko, A., Kawa, S.R., Kato, S., Kumpula, T., Kyrölä, E., Loboda, T.V., McDonald, K.C., Montesano, P.M., Nassar, R., Neigh, C.S.R., Parkinson, C.L., Poulter, B., Pulliainen, J., Rautiainen, K., Rogers, B.M., Rousseaux, C.S., Soja, A.J., Steiner, N., Tamminen, J., Taylor, P.C., Tzortziou, M.A., Virta, H., Wang, J.S., Watts, J.D., Winker, D.M., Wu, D.L., 2020. Space-based observations for understanding changes in the Arctic-Boreal Zone. *Rev. Geophys.* 58, e2019RG000652 <https://doi.org/10.1029/2019RG000652>.
- EU, 2000. Water Framework Directive - European Commission [WWW Document]. URL [https://environment.ec.europa.eu/topics/water/water-framework-directive\\_en](https://environment.ec.europa.eu/topics/water/water-framework-directive_en) (accessed 2.1.24).
- EU, 2021. Soil strategy for 2023 - European Commission [WWW Document]. URL [https://environment.ec.europa.eu/topics/soil-and-land/soil-strategy\\_en#objectives](https://environment.ec.europa.eu/topics/soil-and-land/soil-strategy_en#objectives) (accessed 1.4.24).
- Fassnacht, F.E., Stenzel, S., Gitelson, A.A., 2015. Non-destructive estimation of foliar carotenoid content of tree species using merged vegetation indices. *J. Plant Physiol.* 176, 210–217. <https://doi.org/10.1016/j.jplph.2014.11.003>.
- Feilhauer, H., Schmid, T., Faude, U., Sánchez-Carrillo, S., Cirujano, S., 2018. Are remotely sensed traits suitable for ecological analysis? A case study of long-term drought effects on leaf mass per area of wetland vegetation. *Ecol. Indic.* 88, 232–240. <https://doi.org/10.1016/j.ecolind.2018.01.012>.
- Feilhauer, H., Zlinszky, A., Kania, A., Foody, G.M., Doktor, D., Lausch, A., Schmidlein, S., 2021. Let your maps be fuzzy!—class probabilities and floristic gradients as alternatives to crisp mapping for remote sensing of vegetation. *Remote Sens. Ecol. Conserv.* 7, 292–305. <https://doi.org/10.1002/rse2.188>.
- Féret, J.B., Gitelson, A.A., Noble, S.D., Jacquemoud, S., 2017. PROSPECT-D: towards modeling leaf optical properties through a complete lifecycle. *Remote Sens. Environ.* 193, 204–215. <https://doi.org/10.1016/j.rse.2017.03.004>.
- Féret, J.B., Berger, K., de Boissieu, F., Malenovsky, Z., 2021. PROSPECT-PRO for estimating content of nitrogen-containing leaf proteins and other carbon-based constituents. *Remote Sens. Environ.* 252, 112173 <https://doi.org/10.1016/j.rse.2020.112173>.
- Foerster, S., Carrère, V., Rast, M., Staenz, K., 2016. Preface: the environmental mapping and analysis program (EnMAP) Mission: preparing for its scientific exploitation. *Remote Sens.* 8, 957. <https://doi.org/10.3390/RS8110957>.
- Foerster, S., Brosinsky, A., Koch, K., Eckardt, R., 2024. HYPERedu online learning program for hyperspectral remote sensing: concept, implementation and lessons learned. *Int. J. Appl. Earth Obs. Geoinf.* 131, 103983 <https://doi.org/10.1016/j.jag.2024.103983>.
- Gamon, J.A., Serrano, L., Surfus, J.S., 1997. The photochemical reflectance index: an optical indicator of photosynthetic radiation use efficiency across species, functional types, and nutrient levels. *Oecologia* 112, 492–501. <https://doi.org/10.1007/S004420050337>.
- Gasela, M., Kganyago, M., De Jager, G., 2022. Testing the utility of the resampled nSight-2 spectral configurations in discriminating wetland plant species using random Forest classifier. *Geocarto Int.* <https://doi.org/10.1080/10106049.2022.2060326>.
- Giardino, C., Brando, V.E., Gege, P., Pinnel, N., Hochberg, E., Knaeps, E., Reusen, I., Doerffer, R., Bresciani, M., Braga, F., Foerster, S., Champollion, N., Dekker, A., 2019. Imaging spectrometry of inland and coastal waters: state of the art, achievements and perspectives. *Surv. Geophys.* 40, 401–429. <https://doi.org/10.1007/S10712-018-9476-0>.
- Gitelson, A.A., Keydan, G.P., Merzlyak, M.N., 2006. Three-band model for noninvasive estimation of chlorophyll, carotenoids, and anthocyanin contents in higher plant leaves. *Geophys. Res. Lett.* 33 <https://doi.org/10.1029/2006GL026457>.
- Goetz, A.F.H., 2009. Three decades of hyperspectral remote sensing of the earth: A personal view. *Remote Sens. Environ.* 113, S5–S16. <https://doi.org/10.1016/j.rse.2007.12.014>.
- Goetz, A.F.H., Vane, G., Solomon, J.E., Rock, B.N., 1985. Imaging spectrometry for earth remote sensing. *Science* 179 (228), 1147–1153. <https://doi.org/10.1126/SCIENCE.228.4704.1147>.
- Goetz, A.F.H., Chabrilat, S., Lu, Z., 2001. Field reflectance spectrometry for detection of swelling clays at construction sites. *Field Anal. Chem. Technol.* 5, 143–155. <https://doi.org/10.1002/FACT.1015>.
- Green, R.O., 2022. The NASA Earth Venture Instrument, Earth Surface Mineral Dust Source Investigation (EMIT). *International Geoscience and Remote Sensing Symposium (IGARSS) 2022-July*, pp. 5004–5006. <https://doi.org/10.1109/IGARSS46834.2022.9883479>.
- Guanter, L., Gómez-Chova, L., Moreno, J., 2008. Coupled retrieval of aerosol optical thickness, columnar water vapor and surface reflectance maps from ENVISAT/MERIS data over land. *Remote Sens. Environ.* 112, 2898–2913. <https://doi.org/10.1016/j.rse.2008.02.001>.
- Guanter, L., Kaufmann, H., Segl, K., Foerster, S., Rogass, C., Chabrilat, S., Kuester, T., Hollstein, A., Rossner, G., Chlebek, C., Straif, C., Fischer, S., Schrader, S., Storch, T., Heiden, U., Mueller, A., Bachmann, M., Mühle, H., Müller, R., Habermeyer, M., Ohndorf, A., Hill, J., Buddenbaum, H., Hostert, P., Van Der Linden, S., Leitão, P.J., Rabe, A., Doerffer, R., Krasemann, H., Xi, H., Mauser, W., Hank, T., Locherer, M., Rast, M., Staenz, K., Sang, B., 2015. The EnMAP spaceborne imaging spectroscopy mission for earth observation. *Remote Sens.* 7, 8830–8857. <https://doi.org/10.3390/RS70708830>.
- Guanter, L., Brell, M., Chan, J.C.W., Giardino, C., Gomez-Dans, J., Mielke, C., Morsdorf, F., Segl, K., Yokoya, N., 2019. Synergies of spaceborne imaging spectroscopy with other remote sensing approaches. *Surv. Geophys.* 40, 657–687. <https://doi.org/10.1007/S10712-018-9485-Z>.
- Guanter, L., Irakulis-Loitxate, I., Gorroño, J., Sánchez-García, E., Cusworth, D.H., Varon, D.J., Cogliati, S., Colombo, R., 2021. Mapping methane point emissions with the PRISMA spaceborne imaging spectrometer. *Remote Sens. Environ.* 265, 112671 <https://doi.org/10.1016/j.rse.2021.112671>.
- Hank, T.B., Berger, K., Bach, H., Clevers, J.G.P.W., Gitelson, A., Zarco-Tejada, P., Mauser, W., 2019. Spaceborne imaging spectroscopy for sustainable agriculture: contributions and challenges. *Surv. Geophys.* 40, 515–551. <https://doi.org/10.1007/S10712-018-9492-0>.
- Hestir, E.L., Brando, V.E., Bresciani, M., Giardino, C., Matta, E., Villa, P., Dekker, A.G., 2015. Measuring freshwater aquatic ecosystems: the need for a hyperspectral global mapping satellite mission. *Remote Sens. Environ.* 167, 181–195. <https://doi.org/10.1016/j.rse.2015.05.023>.
- Hill, J., Buddenbaum, H., Townsend, P.A., 2019. Imaging spectroscopy of forest ecosystems: perspectives for the use of spaceborne hyperspectral earth observation systems. *Surv. Geophys.* 40, 553–588. <https://doi.org/10.1007/s10712-019-09514-2>.
- IGKB, 2024. Jahresbericht der Internationalen Gewässerschutzkommission für den Bodensee: Limnologischer Zustand des Bodensees (in preparation).
- IPCC, 2022. Summary for Policy Makers, in: *Climate Change 2022: Impacts, Adaptation and Vulnerability*. Cambridge University Press, Cambridge, UK and New York, NY, USA, pp. 3–33. <https://doi.org/10.1017/9781009325844.001>.
- Jacquemoud, S., Baret, F., 1990. PROSPECT: a model of leaf optical properties spectra. *Remote Sens. Environ.* 34 (2), 75–91. [https://doi.org/10.1016/0034-4257\(90\)90100-Z](https://doi.org/10.1016/0034-4257(90)90100-Z).
- Jacquemoud, S., Verhoef, W., Baret, F., Bacour, C., Zarco-Tejada, P.J., Asner, G.P., François, C., Ustin, S.L., 2009. PROSPECT + SAIL models: a review of use for vegetation characterization. *Remote Sens. Environ.* 113, S56–S66. <https://doi.org/10.1016/j.rse.2008.01.026>.
- Jakimow, B., Janz, A., Thiel, F., Okujeni, A., Hostert, P., van der Linden, S., 2023. EnMAP-Box: imaging spectroscopy in QGIS. *SoftwareX* 23. <https://doi.org/10.1016/j.softx.2023.101507>.
- Jänicke, C., Okujeni, A., Cooper, S., Clark, M., Hostert, P., van der Linden, S., 2020. Brightness gradient-corrected hyperspectral image mosaics for fractional vegetation cover mapping in northern California. *Remote Sens. Lett.* 11, 1–10. <https://doi.org/10.1080/2150704X.2019.1670518>.
- Jay, S., Bendoula, R., Hadoux, X., Féret, J.-B., Goretta, N., 2016. A physically-based model for retrieving foliar biochemistry and leaf orientation using close-range imaging spectroscopy. *Remote Sens. Environ.* 177, 220–236. <https://doi.org/10.1016/j.rse.2016.02.029>.
- Jędrzych, M., Zagajewski, B., Marcinkowska-Ochtyra, A., 2017. Application of Sentinel-2 and EnMAP new satellite data to the mapping of alpine vegetation of the Karkonosze Mountains. *Polish Cartograph. Rev.* 49, 107–119. <https://doi.org/10.1515/PCR-2017-0011>.
- Kamoske, A.G., Dahlin, K.M., Read, Q.D., Record, S., Stark, S.C., Serbin, S.P., Zarnetske, P.L., 2022. Towards mapping biodiversity from above: can fusing lidar and hyperspectral remote sensing predict taxonomic, functional, and phylogenetic tree diversity in temperate forests? *Glob. Ecol. Biogeogr.* 31, 1440–1460. <https://doi.org/10.1111/GEB.13516>.
- Kaufmann, H., Sang, B., Storch, T., Segl, K., Foerster, S., Guanter, L., Erhard, M., Heider, B., Hofer, S., Honold, H.P., Penné, B., Bachmann, M., Habermeyer, M., Müller, A., Müller, R., Rast, M., Staenz, K., Straif, C., Chlebek, C., 2015. Environmental mapping and analysis program - A German hyperspectral mission. *Optical Payloads for Space Missions*. <https://doi.org/10.1002/9781118945179.ch7>.
- Kokhanovsky, A., Vandecrux, B., Wehrle, A., Danne, O., Brockmann, C., Box, J.E., 2023a. An improved retrieval of snow and ice properties using spaceborne OLCI/S-3 spectral reflectance measurements: updated atmospheric correction and snow impurity load estimation. *Remote Sens.* 15, 77. <https://doi.org/10.3390/RS15010077>.
- Kokhanovsky, A.A., Brell, M., Segl, K., Bianchini, G., Lanconelli, C., Lupi, A., Petkov, B., Picard, G., Arnaud, L., Stone, R.S., Chabrilat, S., 2023b. First retrievals of surface and atmospheric properties using EnMAP measurements over Antarctica. *Remote Sens.* 15, 3042. <https://doi.org/10.3390/RS15123042>.

- Kyriou, A., Nikolakopoulos, K., 2020. Landslide mapping using optical and radar data: a case study from Aminteo, Western Macedonia Greece. *Eur. J. Remote Sens.* 53, 17–27. <https://doi.org/10.1080/22797254.2019.1681905>.
- Liu, Y.-N., Zhang, J., Zhang, Y., Sun, W.-W., Jiao, L.-L., Sun, D.-X., Hu, X.-N., Ye, X., Li, Y.-D., Liu, S.-F., Cao, K.-Q., Chai, M.-Y., Zhou, W.-Y.-N., 2019. The advanced hyperspectral imager: aboard China's GaoFen-5 satellite. *IEEE Geosci. Remote Sens. Mag.* 7 (4), 23–32. <https://doi.org/10.1109/MGRS.2019.2927687>.
- Locherer, M., Hank, T., Danner, M., Mauser, W., 2015. Retrieval of seasonal leaf area index from simulated EnMAP data through optimized LUT-based inversion of the PROSAIL model. *Remote Sens.* 7 (8), 10321–10346. <https://doi.org/10.3390/rs70810321>.
- Lopinto, E., Fasano, L., Longo, F., Sacco, P., 2022. Current Status of Prisma Mission. *International Geoscience and Remote Sensing Symposium (IGARSS) 2022-July*, pp. 5389–5390. <https://doi.org/10.1109/IGARSS46834.2022.9884414>.
- Marcinkowska-Ochtyra, A., Zagajewski, B., Ochtyra, A., Jaroćńska, A., Wojtuń, B., Rogas, C., Mielke, C., Lavender, S., 2017. Subalpine and alpine vegetation classification based on hyperspectral APEX and simulated EnMAP images. *Int. J. Remote Sens.* 38, 1839–1864. <https://doi.org/10.1080/01431161.2016.1274447>.
- Matsunaga, T., Iwasaki, A., Tachikawa, T., Tani, J., Kashimura, O., Mouri, K., Inada, H., Tsuchida, S., Nakamura, R., Yamamoto, H., Iwao, K., 2022. The Status and Early Results of Hyperspectral Imager Suite (HISUI). *International Geoscience and Remote Sensing Symposium (IGARSS) 2022-July*, pp. 5399–5400. <https://doi.org/10.1109/IGARSS46834.2022.9883526>.
- Milewski, R., Chabrilat, S., Bookhagen, B., 2020. Analyses of Namibian seasonal salt pan crust dynamics and climatic drivers using Landsat 8 time-series and ground data. *Remote Sens.* 12, 474. <https://doi.org/10.3390/rs12030474>.
- Milewski, R., Schmid, T., Chabrilat, S., Jiménez, M., Escribano, P., Pelayo, M., Bendor, E., 2022. Analyses of the impact of soil conditions and soil degradation on vegetation vitality and crop productivity based on airborne hyperspectral VNIR–SWIR–TIR data in a semi-arid rainfed agricultural area (Camarena, Central Spain). *Remote Sens.* 14, 5131. <https://doi.org/10.3390/rs14205131>.
- Murphy, F., Schmieder, K., Baastrop-Spohr, L., Pedersen, O., Sand-Jensen, K., 2018. Five decades of dramatic changes in submerged vegetation in Lake Constance. *Aquat. Bot.* 144, 31–37. <https://doi.org/10.1016/j.aquabot.2017.10.006>.
- National Academies of Sciences, Engineering, and Medicine, 2018. *Thriving on Our Changing Planet: A Decadal Strategy for Earth Observation from Space, Thriving on Our Changing Planet*. National Academies Press. <https://doi.org/10.17226/24938>.
- Niroumand-Jadidi, M., Bovolo, F., Bruzzone, L., 2020. Water quality retrieval from PRISMA hyperspectral images: first experience in a turbid lake and comparison with Sentinel-2. *Remote Sens.* 12, 3984. <https://doi.org/10.3390/rs12233984>.
- Numata, I., Cochrane, M.A., Jr., C.M.S., Sales, M.H., 2011. Carbon emissions from deforestation and forest fragmentation in the Brazilian Amazon. *Environ. Res. Lett.* 6, 44003. <https://doi.org/10.1088/1748-9326/6/4/044003>.
- Nurda, N., Noguchi, R., Ahamed, T., 2020. Forest productivity and carbon stock analysis from vegetation phenological indices using satellite remote sensing in Indonesia. *Asia Pac. J. Reg. Sci.* 4, 657–690. <https://doi.org/10.1007/s41685-020-00163-7>.
- Okujeni, A., Jänicke, C., Cooper, S., Frantz, D., Hostert, P., Clark, M., Segl, K., van der Linden, S., 2021. Multi-season unmixing of vegetation class fractions across diverse Californian ecoregions using simulated spaceborne imaging spectroscopy data. *Remote Sens. Environ.* 264, 112558. <https://doi.org/10.1016/j.rse.2021.112558>.
- Ollinger, S., 2011. Sources of variability in canopy reflectance and the convergent properties of plants. *New Phytol.* 189, 375–394. <https://doi.org/10.1111/j.1469-8137.2010.03536.x>.
- Ong, C.C.H., 2013. *Mapping and Monitoring the Environmental Impacts of Mining Using Hyperspectral Data, in Department of Imaging and Applied Physics. Curtin University of Technology, Perth, Western Australia*, p. 250.
- Ong, C.C.H., Cudahy, T.J., 2014. Mapping contaminated soils: using remotely-sensed hyperspectral data to predict pH. *Eur. J. Soil Sci.* 65, 897–906. <https://doi.org/10.1111/EJSS.12160>.
- Ong, C.C.H., Cudahy, T.J., Caccetta, M.S., Piggott, M.S., 2003. Deriving quantitative dust measurements related to iron ore handling from airborne hyperspectral data. *Min. Technol.* 112. <https://doi.org/10.1179/037178403225003555>.
- Painter, T.H., Seidel, F.C., Bryant, A.C., McKenzie Skiles, S., Rittger, K., 2013. Imaging spectroscopy of albedo and radiative forcing by light-absorbing impurities in mountain snow. *J. Geophys. Res. Atmos.* 118, 9511–9523. <https://doi.org/10.1002/jgrd.50520>.
- Pearlman, J.S., Barry, P.S., Segal, C.C., Shepanski, J., Beiso, D., Carman, S.L., 2003. Hyperion, a space-based imaging spectrometer. *IEEE Trans. Geosci. Remote Sens.* 41, 1160–1173. <https://doi.org/10.1109/TGRS.2003.815018>.
- Pereira, H.M., Ferrier, S., Walters, M., Geller, G.N., Jongman, R.H.G., Scholes, R.J., Bruford, M.W., Brummitt, N., Butchart, S.H.M., Cardoso, A.C., Coops, N.C., Dulloo, E., Faith, D.P., Freyhof, J., Gregory, R.D., Heip, C., Hoft, R., Hurtt, G., Jetz, W., Karp, D.S., McGeoch, M.A., Obura, D., Onoda, Y., Pettorelli, N., Reyers, B., Sayre, R., Scharlemann, J.P.W., Stuart, S.N., Turak, E., Walpole, M., Wegmann, M., 2013. Essential biodiversity variables. *Science* (1979) 339, 277–278. <https://doi.org/10.1126/science.1229931>.
- Petri, M., 2006. Water quality of lake constance. In: Knepper, T.P. (Ed.), *The Rhine. The Handbook of Environmental Chemistry*. Springer, Berlin, Heidelberg, pp. 127–138. [https://doi.org/10.1007/978-3-540-01818-1\\_10](https://doi.org/10.1007/978-3-540-01818-1_10).
- Post, E., Forchhammer, M.C., Bret-Harte, M.S., Callaghan, T.V., Christensen, T.R., Elberling, B., Fox, A.D., Gilg, O., Hik, D.S., Høye, T.T., Ims, R.A., Jeppesen, E., Klein, D.R., Madsen, J., McGuire, A.D., Rysgaard, S., Schindler, D.E., Stirling, I., Tamstorf, M.P., Tyler, N.J.C., Van Der Wal, R., Welker, J., Wookey, P.A., Schmidt, N.M., Aastrup, P., 2009. Ecological dynamics across the arctic associated with recent climate change. *Science* 1979 (325), 1355–1358. <https://doi.org/10.1126/science.1173113>.
- Prevéj, J., Vellend, M., Rüger, N., Hollister, R.D., Bjorkman, A.D., Myers-Smith, I.H., Elmendorf, S.C., Clark, K., Cooper, E.J., Elberling, B., Fosaa, A.M., Henry, G.H.R., Høye, T.T., Jónsdóttir, I.S., Klanderud, K., Lévesque, E., Mauritz, M., Molau, U., Natali, S.M., Oberbauer, S.F., Panchen, Z.A., Post, E., Rumpf, S.B., Schmidt, N.M., Schuur, E.A.G., Semenchuk, P.R., Troxler, T., Welker, J.M., Rixen, C., 2017. Greater temperature sensitivity of plant phenology at colder sites: implications for convergence across northern latitudes. *Glob. Chang. Biol.* 23, 2660–2671. <https://doi.org/10.1111/gcb.13619>.
- Rasmussen, C.E., Williams, C.K.I., 2006. *Gaussian Processes for Machine Learning. Adaptive Computation and Machine Learning*. MIT Press, Cambridge, Mass.
- Richter, N., Staenz, K., Kaufmann, H., 2008. Spectral unmixing of airborne hyperspectral data for baseline mapping of mine tailings areas. *Int. J. Remote Sens.* 29, 3937–3956. <https://doi.org/10.1080/01431160801891788>.
- Roberts, D.A., Bradley, E.S., Cheung, R., Leifer, I., Dennison, P.E., Margolis, J.S., 2010. Mapping methane emissions from a marine geological seep source using imaging spectrometry. *Remote Sens. Environ.* 114 (3), 592–606. <https://doi.org/10.1016/j.rse.2009.10.015>.
- Roger, J., Irakulis-Loitxate, I., Valverde, A., Gorroño, J., Chabrilat, S., Brell, M., Guanter, L., 2024. High-resolution methane mapping with the EnMAP satellite imaging spectroscopy mission. *IEEE Trans. Geosci. Remote Sens.* 62, 1–12. <https://doi.org/10.1109/TGRS.2024.3352403>.
- Rogers, A., Medlyn, B.E., Dukles, J.S., Bonan, G., von Caemmerer, S., Dietze, M.C., Kattge, J., Leakey, A.D.B., Mercado, L.M., Niinemets, Ü., Prentice, I.C., Serbin, S.P., Sitch, S., Way, D.A., Zaehle, S., 2017. A roadmap for improving the representation of photosynthesis in earth system models. *New Phytol.* 213, 22–42. <https://doi.org/10.1111/NPH.14283>.
- Sarangi, C., Qian, Y., Rittger, K., Ruby Leung, L., Chand, D., Bormann, K.J., Painter, T.H., 2020. Dust dominates high-altitude snow darkening and melt over high-mountain Asia. *Nat. Clim. Chang.* 10, 1045–1051. <https://doi.org/10.1038/s41558-020-00909-3>.
- Schaepman, M.E., Ustin, S.L., Plaza, A.J., Painter, T.H., Verrelst, J., Liang, S., 2009. Earth system science related imaging spectroscopy—an assessment. *Remote Sens. Environ.* 113, S123–S137. <https://doi.org/10.1016/j.rse.2009.03.001>.
- Schlerf, M., Atzberger, C., Hill, J., Buddenbaum, H., Werner, W., Schüller, G., 2010. Retrieval of chlorophyll and nitrogen in Norway spruce (*Picea abies* L. Karst.) using imaging spectroscopy. *Int. J. Appl. Earth Obs. Geoinf.* 12, 17–26. <https://doi.org/10.1016/j.jag.2009.08.006>.
- Schodlak, M.C., Frei, M., Segl, K., 2022. Implications of new hyperspectral satellites for rock materials exploration. *Miner. Econ.* 35, 495–502. <https://doi.org/10.1007/S13563-022-00327-1>.
- Schwieder, M., Leitão, P.J., Suess, S., Senf, C., Hostert, P., 2014. Estimating fractional shrub cover using simulated EnMAP data: a comparison of three machine learning regression techniques. *Remote Sens.* 6, 3427–3445. <https://doi.org/10.3390/rs6043427>.
- Skidmore, A.K., Pettorelli, N., Coops, N.C., Geller, G.N., Hansen, M., Lucas, R., Múcher, C.A., O'Connor, B., Paganini, M., Pereira, H.M., Schaepman, M.E., Turner, W., Wang, T., Wegmann, M., 2015. Environmental science: agree on biodiversity metrics to track from space. *Nature* 523, 403–405. <https://doi.org/10.1038/523403a>.
- Skidmore, A.K., Coops, N.C., Neinavaz, E., Ali, A., Schaepman, M.E., Paganini, M., Kissling, W.D., Vihervaara, P., Davishzadeh, R., Feilhauer, H., Fernandez, M., Fernández, N., Gorelick, N., Geijzendorffer, I., Heiden, U., Heurich, M., Hobern, D., Holzwarth, S., Müller-Karger, F.E., Van De Kerchove, R., Lausch, A., Leitão, P.J., Lock, M.C., Múcher, C.A., O'Connor, B., Rocchini, D., Roeoeli, C., Turner, W., Vis, J. K., Wang, T., Wegmann, M., Wingate, V., 2021. Priority list of biodiversity metrics to observe from space. *Nat. Ecol. Evol.* 5, 896–906. <https://doi.org/10.1038/s41559-021-01451-x>.
- Skiles, S.M.K., Flanner, M., Cook, J.M., Dumont, M., Painter, T.H., 2018. Radiative forcing by light-absorbing particles in snow. *Nat. Clim. Chang.* 8, 964–971. <https://doi.org/10.1038/s41558-018-0296-5>.
- Sonobe, R., Wang, Q., 2018. Nondestructive assessments of carotenoids content of broadleaved plant species using hyperspectral indices. *Comput. Electron. Agric.* 145, 18–26. <https://doi.org/10.1016/j.compag.2017.12.022>.
- Soppa, M.A., Silva, B., Steinmetz, F., Keith, D., Scheffler, D., Bohn, N., Bracher, A., 2021. Assessment of polymer atmospheric correction algorithm for hyperspectral remote sensing imagery over coastal waters. *Sensors* 21, 4125. <https://doi.org/10.3390/S21124125>.
- Steinmetz, F., Deschamps, P.-Y., Ramon, D., 2011. Atmospheric correction in presence of sun glint: application to MERIS. *Opt. Express* 19 (10), 9783–9800. <https://doi.org/10.1364/OE.19.009783>.
- Storch, T., Honold, H.P., Chabrilat, S., Habermeyer, M., Tucker, P., Brell, M., Ohndorf, A., Wirth, K., Betz, M., Kuchler, M., Mühle, H., Carmona, E., Baur, S., Mücke, M., Löw, S., Schulze, D., Zimmermann, S., Lenzen, C., Wiesner, S., Aida, S., Kahle, R., Willburger, P., Hartung, S., Dietrich, D., Plesia, N., Tegler, M., Schork, K., Alonso, K., Marshall, D., Gerasch, B., Schwind, P., Pato, M., Schneider, M., de los Reyes, R., Langheinrich, M., Wenzel, J., Bachmann, M., Holzwarth, S., Pinnel, N., Guanter, L., Segl, K., Scheffler, D., Foerster, S., Bohn, N., Bracher, A., Soppa, M.A., Gascon, F., Green, R., Kokaly, R., Moreno, J., Ong, C., Sornig, M., Wernitz, R., Bagschik, K., Reintsema, D., La Porta, L., Schickling, A., Fischer, S., 2023. The EnMAP imaging spectroscopy mission towards operations. *Remote Sens. Environ.* 294, 113632. <https://doi.org/10.1016/j.rse.2023.113632>.
- Suess, S., Van Der Linden, S., Okujeni, A., Leitão, P.J., Schwieder, M., Hostert, P., 2015. Using class probabilities to map gradual transitions in shrub vegetation from simulated EnMAP data. *Remote Sens.* 7, 10668–10688. <https://doi.org/10.3390/rs70810668>.

- Swayze, G.A., Smith, K.S., Clark, R.N., Sutley, S.J., Pearson, R.M., Vance, J.S., Hageman, P.L., Briggs, P.H., Meier, A.L., Singleton, M.J., Roth, S., 2000. Using imaging spectroscopy to map acidic mine waste. *Environ. Sci. Technol.* 34, 47–54. <https://doi.org/10.1021/es990046w>.
- Thompson, D.R., Thorpe, A.K., Frankenberg, C., Green, R.O., Duren, R., Guanter, L., Hollstein, A., Middleton, E., Ong, L., Ungar, S., 2016. Space-based remote imaging spectroscopy of the Aliso canyon CH<sub>4</sub> superemitter. *Geophys. Res. Lett.* 43, 6571–6578. <https://doi.org/10.1002/2016GL069079>.
- Thorpe, A.K., Frankenberg, C., Thompson, D.R., Duren, R.M., Aubrey, A.D., Bue, B.D., Green, R.O., Gerilowski, K., Krings, T., Borchardt, J., Kort, E.A., Sweeney, C., Conley, S., Roberts, D.A., Dennison, P.E., 2017. Airborne DOAS retrievals of methane, carbon dioxide, and water vapor concentrations at high spatial resolution: application to AVIRIS-NG. *Atmos. Meas. Tech.* 10, 3833–3850. <https://doi.org/10.5194/amt-10-3833-2017>.
- Turpie, K.R., Casey, K.A., Crawford, C.J., Guild, L.S., Kieffer, H., Lin, G., Kokaly, R., Shrestha, A.K., Anderson, C., Ramaseri Chandra, S.N., Green, R., Hook, S., Lukashin, C., Thome, K., 2023. Calibration and validation for the surface biology and geology (SBG) Mission concept: recommendations for a multi-sensor system for imaging spectroscopy and thermal imagery. *Eur. J. Vasc. Endovasc. Surg.* 128 <https://doi.org/10.1029/2023JG007452>.
- UN, 2016. THE 17 GOALS | Sustainable Development [WWW Document]. URL: <https://sdgs.un.org/goals> (accessed 1.26.24).
- van den Broeke, M., Box, J., Fettweis, X., Hanna, E., Noël, B., Tedesco, M., van As, D., van de Berg, W.J., van Kampenhout, L., 2017. Greenland ice sheet surface mass loss: recent developments in observation and modeling. *Curr. Clim. Chang. Rep.* 3, 345–356. <https://doi.org/10.1007/S40641-017-0084-8>.
- Van Der Linden, S., Rabe, A., Held, M., Jakimow, B., Leitão, P.J., Okujeni, A., Schwieder, M., Suess, S., Hostert, P., Rast, M., Foerster, S., Carrere, V., Staenz, K., Galvao, S., Müller, R., Thenkabail, P.S., 2015. The EnMAP-Box—A toolbox and application programming interface for EnMAP data processing. *Remote Sens.* 7, 11249–11266. <https://doi.org/10.3390/RS70911249>.
- Van Wesemael, B., Chabrillat, S., 2023. Remote sensing of soil organic carbon. In: Goss, M.J., Oliver, M.A. (Eds.), *Encyclopedia of Soils in the Environment*. Elsevier.
- Verhoef, W., Jia, L., Xiao, Q., Su, Z., 2007. Unified optical-thermal four-stream radiative transfer theory for homogeneous vegetation canopies. *IEEE Trans. Geosci. Remote Sens.* 45 (6), 1808–1822. <https://doi.org/10.1109/tgrs.2007.895844>.
- Verrelst, J., Halabuk, A., Atzberger, C., Hank, T., Steinhauser, S., Berger, K., 2023. A comprehensive survey on quantifying non-photosynthetic vegetation cover and biomass from imaging spectroscopy. *Ecol. Indic.* 155, 110911 <https://doi.org/10.1016/J.ECOLIND.2023.110911>.
- Wang, Z., Skidmore, A.K., Darvishzadeh, R., Wang, T., 2018. Mapping forest canopy nitrogen content by inversion of coupled leaf-canopy radiative transfer models from airborne hyperspectral imagery. *Agric. For. Meteorol.* 253–254, 247–260. <https://doi.org/10.1016/J.AGRFORMET.2018.02.010>.
- West, J., 2020. Extractable global resources and the future availability of metal stocks: “known unknowns” for the foreseeable future. *Res. Policy* 65, 101574. <https://doi.org/10.1016/J.RESOURPOL.2019.101574>.
- Woche, M., Berger, K., Danner, M., Mauser, W., Hank, T., 2018. Physically-based retrieval of canopy equivalent water thickness using hyperspectral data. *Remote Sens.* 10, 1924. <https://doi.org/10.3390/RS10121924>.
- Woche, M., Berger, K., Danner, M., Mauser, W., Hank, T., 2020. RTM-based dynamic absorption integrals for the retrieval of biochemical vegetation traits. *Int. J. Appl. Earth Obs. Geoinf.* 93, 102219 <https://doi.org/10.1016/j.jag.2020.102219>.
- Woche, M., Berger, K., Verrelst, J., Hank, T., 2022. Retrieval of carbon content and biomass from hyperspectral imagery over cultivated areas. *ISPRS J. Photogramm. Remote Sens.* 193, 104–114. <https://doi.org/10.1016/j.isprsjprs.2022.09.003>.
- Wrona, F.J., Johansson, M., Culp, J.M., Jenkins, A., Mård, J., Myers-Smith, I.H., Prowse, T.D., Vincent, W.F., Wookey, P.A., 2016. Transitions in Arctic ecosystems: ecological implications of a changing hydrological regime. *Eur. J. Vasc. Endovasc. Surg.* 121, 650–674. <https://doi.org/10.1002/2015JG003133>.
- Xiao, J., Chevallier, F., Gomez, C., Guanter, L., Hicke, J.A., Huete, A.R., Ichii, K., Ni, W., Pang, Y., Rahman, A.F., Sun, G., Yuan, W., Zhang, L., Zhang, X., 2019. Remote sensing of the terrestrial carbon cycle: a review of advances over 50 years. *Remote Sens. Environ.* 233, 111383 <https://doi.org/10.1016/J.RSE.2019.111383>.
- Zabci, N., Rivard, B., Ong, C., Mueller, A., 2014. Using airborne hyperspectral data to characterize the surface pH and mineralogy of pyrite mine tailings. *Int. J. Appl. Earth Obs. Geoinf.* 32, 152–162. <https://doi.org/10.1016/J.JAG.2014.04.008>.
- Zhang, Y., Migliavacca, M., Penuelas, J., Ju, W., 2021. Advances in hyperspectral remote sensing of vegetation traits and functions. *Remote Sens. Environ.* 252, 112121 <https://doi.org/10.1016/J.RSE.2020.112121>.